$\begin{array}{c} \textbf{Acceleration of Polarized Protons} \\ \textbf{to 820 GeV at HERA}^* \end{array}$

SPIN Collaboration

Michigan, Indiana, IHEP-Protvino JINR-Dubna, Moscow, INR-Moscow, BINP-Novosibirsk KEK, TRIUMF

DESY Polarization Team

The SPIN Collaboration and the DESY Polarization Team have studied the possible acceleration of a polarized proton beam to 820 GeV/c in the HERA accelerator complex at DESY. The main problems which need further study are:

- increasing the accumulated polarized proton intensity,
- providing adequate spin stability with four or more Siberian snakes in HERA.

All other problems appear to have straightforward solutions using existing techniques. The first Section of this Report summarizes the changes needed in each accelerator for polarized proton acceleration; it also contains a possible Schedule and Budget for the polarized proton beam project. The rest of the Report describes a possible plan to accelerate polarized protons and to perform polarized proton experiments at 820 GeV/c.

TABLE OF CONTENTS

3
9
15
23
33
39
45
51
57
69
77
81
87

 $[^]st$ Supported by research grants from DESY and the U.S. Department of Energy

SPIN@HERA Collaboration

- L.V. Alexeeva^a, V. A. Anferov, B. B. Blinov, J. A. Bywater, D. D. Caussyn^b, E. D. Courant^c,
- D. G. Crabb^d, D. A. Crandell, Ya. S. Derbenev^e, S. E. Gladycheva, F. Z. Khiari^f, S. V. Koutin,
- A. D. Krisch, A. M. T. Lin, T. J. Liu, W. Lorenzon, V. G. Luppov, D. C. Peaslee, R. A. Phelps,
- G. P. Ramsey^g, L. G. Ratner, R. S. Raymond, D. S. Shoumkin^a, J. A. Stewart^h, S. M. Varzar^a, V. K. Wong
- THE UNIVERSITY OF MICHIGAN, ANN ARBOR, U.S.A.
- J. M. Cameron, C. M. Chu, T. B. Cleggⁱ, V.P. Derenchuk, D. L. Friesel, S. Y. Lee, M. G. Minty^j, T. Rinckel, P. Schwandt, J. Sowinski, F. Sperisen, E. J. Stephenson, B. von Przewoski
- INDIANA UNIVERSITY CYCLOTRON FACILITY, BLOOMINGTON, U.S.A.
- Yu. M. Ado, P. N. Chirkov, V. N. Grishin, G. G. Gurov, V. A. Kachanov, Yu. V. Kharlov,
- V. Yu. Khodyrev, O. I. Kisly, V. V. Mochalov, S. B. Nurushev, D. I. Patalakha, A. F. Prudkoglyad,
- V. V. Rykalin, V. P. Sakharov, P. A. Semenov, V. L. Solovianov, V. P. Stepanov, L. M. Tkachenko,
- V. A. Teplyakov, S. M. Troshin, N. E. Tyurin, A. G. Ufimtsev, M. N. Ukhanov, A. V. Zherebtsov INSTITUTE OF HIGH ENERGY PHYSICS, PROTVINO, RUSSIA
- V. V. Fimushkin, M. V. Kulikov, V. A. Nikitin, P. V. Nomokonov, A. V. Pavlyuk, Yu. K. Pilipenko, V. B. Shutov
- JOINT INSTITUTE FOR NUCLEAR RESEARCH, DUBNA, RUSSIA
- A. I. Demianov, A. A. Ershov, A. M. Gribushin, N. A. Kruglov, A. S. Proskuryakov,
- A. I. Ostrovidov, L. I. Sarycheva, N. B. Sinejv
- MOSCOW STATE UNIVERSITY, MOSCOW, RUSSIA
- A. S. Belov, L. P. Netchaeva, Yu. V. Plohinskii
- INSTITUTE FOR NUCLEAR RESEARCH, MOSCOW, RUSSIA
- V. I. Davydenko, G. I. Dimov, V. G. Dudnikov
- BUDKER INSTITUTE OF NUCLEAR PHYSICS, NOVOSIBIRSK, RUSSIA
- Y. Mori, C. Ohmori, H. Sato, T. Toyama, K. Yokoya
- KEK & INS-TOYKO, TSUKUBA, JAPAN
- R. Abegg, P.P.J Delheij, G. Dutto, C. D. P. Levy, C.A. Miller, G. Roy^k, T. Sakae^l, P. W. Schmor,
- W. T. H. van Oers, A. N. Zelenski^m
- TRIUMF, VANCOUVER, CANADA
- The spokesperson for the SPIN Collaboration is:
- A. D. Krisch
 Randall Laboratory of Physics
 University of Michigan
 Ann Arbor, Michigan 48109-1120 USA
 Telephone: 313-936-1027
 Telefax: 313-936-0794
 E-mail: KRISCH@umich.edu

Permanent address:

DESY Polarization Team

- D.P. Barber, K. Heinemann, J. Maidment, M. Vogt DESY, HAMBURG, GERMANY
- G. Hoffstätter DARMSTADT UNIVERSITY, DARMSTADT, GERMANY
- V.I. Ptitsin, Yu.M. Shatunov BINP, NOVOSIBIRSK, RUSSIA
- V.V. Balandin, N.I. Golubeva INSTITUTE FOR NUCLEAR RESEARCH, MOSCOW, RUSSIA

1 Introduction and overview

This Report contains a preliminary outline of the steps needed to accelerate a spin-polarized proton beam [1, 2] to 820 GeV/c at the DESY complex. This capability would provide a powerful tool for high energy physics; it would be an appropriate response to the growing interest in spin in high energy physics. Very interesting e^+-e^- polarization results have recently been obtained at SLC [3]; e-p polarization experiments are now being done at HERA [4]; and future p-p polarization experiments have been approved at RHIC [5].

A polarized proton beam in HERA could be used in two modes that could run concurrently. The polarized proton beam could be collided with HERA's existing polarized electron beam at the H-1 and ZEUS collider-detectors to study the spin structure of protons, in particular, the structure function $g_1(x, Q^2)$ at small x values near 10^{-4} . Moreover, the polarized proton beam could be scattered from an internal polarized proton jet target to study both two-spin and one-spin effects in p-p elastic and inclusive cross sections. There is a great deal of interesting physics that could be done with a polarized proton beam at HERA; some of this physics is discussed in Sections 2, 3 and 4 of this Report.

To accelerate polarized protons to 820 GeV/c, changes would be needed in each acceleration stage at DESY, except for the LINAC. These changes are shown in Fig. 1.1, and are discussed in Sections 5–13. However, this Report is certainly not a full design report; several issues will need further study; whenever possible, the different possible options are presented. Some highlights of the proposed polarized proton beam hardware are briefly discussed below.

1.1 Polarized beam acceleration

A state-of-the-art polarized H⁻ ion source must be acquired and installed. This might be either an atomic beam source (ABS), or an optically pumped polarized ion source (OPPIS). Both types of sources are constantly being improved; the best ABS has now achieved a current of 1.0 mA in pulsed operation, while the best OPPIS has recently obtained a DC current of 1.6 mA with an emittance of 2π mm·mrad. These intensities are still well below the present unpolarized source intensity, but they may improve significantly, as discussed in Section 5. Moreover, beam accumulation techniques may significantly increase the polarized beam intensity in HERA, as discussed in Section 13. We hope that, with both source and accumulation improvements, the polarized proton beam intensity in HERA might reach the present unpolarized beam intensity of about 70 mA (10^{13} stored protons) or even the planned unpolarized intensity of 150 mA [6].

The polarized H⁻ ions from the source would be first accelerated to 750 keV by a new RFQ; then they would be accelerated in the then-existing LINAC to either 50 MeV or 160 MeV. Polarimeters installed after the RFQ and the LINAC would monitor the polarization at 750 keV and at the LINAC energy, respectively.

Acceleration through DESY III would require overcoming five strong depolarizing resonances. The one strong and about 13 weak imperfection resonances could be overcome using a solenoidal partial Siberian snake of about 5%, while the four strong intrinsic reso-



nances could be overcome using either conventional tune-shifting pulsed quadrupoles or the new dipole kicker technique. A relative AGS-type internal polarimeter could monitor the polarization up to $7.5~{\rm GeV/c}$.

Two full Siberian snakes would be needed in PETRA to overcome its many strong depolarizing resonances. The snake design is somewhat difficult in PETRA because, at its 7.5 GeV/c injection energy, full Siberian snakes would cause large orbit excursions. We propose that two, either cold or warm, fully-on Siberian snakes should operate in the South proton bypass and in the North straight section. Probably, an AGS-type relative polarimeter, inserted at some short PETRA straight section, would monitor the polarization up to $40 \, \mathrm{GeV/c}$.

Accelerating polarized protons to 820 GeV/c in HERA would require at least four full Siberian snakes. Four superconducting Siberian snakes could easily be located near each of the four long straight sections as shown in Fig. 1.1. However these four snakes may be inadequate to overcome HERA's strong depolarizing resonances and thus provide spin stability. The DESY Polarization team has suggested many ways to further study this possible difficulty which they first discovered using their very detailed spin tracking programs.

It now appears that the four full Siberian snakes suggested for HERA are considerably less effective than the 6 snakes suggested earlier for the Tevatron; the benefit of an odd number of snake pairs was previously used (26 snakes at SSC and 6 snakes at the Tevatron) [7, 1] but perhaps not fully understood. Installing 6 snakes in HERA would probably require replacing some existing HERA dipoles with shorter higher fields dipoles. The questions of depolarizing resonance strengths, spin stability, and the optimum number and orientation of Siberian snakes in HERA certainly require further study.

In addition to the four normal Siberian snakes, four "flattening snakes" should be placed in HERA's North and South collider-detector straight sections to compensate the spin rotation due to the nearby vertical bends. Spin rotators in the North and South Halls could provide any spin orientation for the H1 and ZEUS Detectors. A CNI (Coulomb Nuclear Interference) polarimeter in HERA might give an absolute calibration of the beam polarization up to 820 GeV/c. Simultaneous beam and target measurements of the left-right asymmetry in p-p elastic scattering, using Michigan's polarized jet target in HERA, could check the calibration of the CNI polarimeter. One might also install in HERA a relative AGS-type polarimeter and possibly an inclusive polarimeter. Spin rotators would probably be needed in both the 50 MeV and 40 GeV/c beam transport lines to maintain high polarization.

In summary, two major problems need further study:

- increasing the polarized proton beam intensity by improving both the polarized source and the beam accumulation,
- providing adequate spin stability with four or more full Siberian snakes in HERA.

All other problems appear to have straightforward solutions using existing techniques.

1.2 Schedule

A possible schedule for commissioning the polarized proton beam is estimated in Fig. 1.2. This estimate assumes that the funding for this polarized proton beam project is available now and that no other projects interfere with the commissioning.

Figure 1.2. The schedule for commissioning a polarized proton beam in HERA.

1.3 Budget

The estimated total cost to obtain an 820 GeV/c polarized proton beam capability at DESY is given in 1996 DM. Our estimate of about DM 25 Million seems a quite reasonable investment for the expected physics results. Moreover this cost might be considerably lower if the SPIN Collaboration fabricated some or all of the polarization hardware. However, this estimate assumes that some inexpensive way is found to overcome the possible spin stability problem in HERA with only four Siberian snakes.

Preaccelerator		DM 4.2 M
Polarized H ⁻ ion source	DM 2.7 M	
RFQ and power supply (20 keV to 750 KeV)	DM 0.6 M	
Low energy beam transport, switching magnets, and		
vacuum system	DM 0.6 M	
Building change	DM 0.3 M	
50 MeV LINAC		DM 0.2 M
50 MeV polarimeter (p-Carbon)	DM 0.2 M	
7.5 GeV/c DESY III Booster		DM 0.7 M
Solenoid partial Siberian snake (ramped warm)	DM 0.2 M	
Pulsed quadrupoles or kicker magnets with power supplies	DM 0.3 M	
7.5 GeV/c polarimeter (Relative)	DM 0.2 M	
40 GeV/c PETRA Ring		DM 2.1 M
Two warm Siberian snakes	DM 1.0 M	
Power supplies and connections	DM 0.3 M	
40 GeV/c polarimeters (CNI, Relative, and possibly Inclusive)	DM 0.8 M	
820 GeV/c HERA Ring		DM 8.4 M
4 Superconducting Siberian snakes	DM 2.0 M	
4 Superconducting flattening snakes	DM 2.0 M	
4 Superconducting spin rotators	DM 1.5 M	
Power supplies and cryogenic connections	DM 1.5 M	
820 GeV/c polarimeters (CNI, Inclusive, Relative, Elastic)	DM 1.1 M	
Spin Flippers	DM 0.3 M	
Miscellaneous		DM 1.7 M
Transfer line spin rotators	DM 0.5 M	
Computers, control modules, cables, and interface	DM 1.2 M	
Accelerator Subtotal		DM 17.3 M
Contingency (25%)		DM 4.3 M
ACCELERATOR TOTAL		DM 21.6 M
HERA Internal Target Experiment	DM 2.5 M	
Install Mark-II polarized Jet and spectrometer		
SPIN Experiment subtotal		DM 2.5 M
Contingency (25%)		DM 0.6 M
SPIN EXPERIMENT TOTAL		DM 3.1 M
GRAND TOTAL		DM 24.7 M

1.4 Physics goals

It has recently become more clear that spin effects in high energy collisions provide crucial information about the properties of the elementary particles and their fundamental interactions. Section 2 briefly outlines the experimental data which show that surprisingly large hadronic spin effects persist to the highest measured energies. An 820 GeV/c spin-polarized proton beam at HERA would allow important studies, such as: searches for new particles; direct and unambiguous tests of perturbative QCD; tests of nonperturbative QCD; and measurements of the transverse and longitudinal spin structure of the nucleon.

A major justification for accelerating polarized protons in HERA is their use in fully polarized e-p collisions using the existing HERA 27.5 GeV/c polarized electron beam and the existing H-1 and ZEUS detectors. Since most members of our SPIN Collaboration are not very experienced in e-p collisions, we will not attempt a detailed analysis of how these studies would be aided by proton polarization. Many members of the existing DESY community are much more qualified to make this evaluation.

The SPIN Collaboration is particularly interested in studying one-spin and two-spin effects in proton-proton elastic scattering, and in the inclusive production of π 's, K's, p's, and hyperons. These experiments could be done in the East Hall by colliding HERA's 820 GeV/c polarized proton beam with the Michigan ultra-cold proton-spin-polarized atomic hydrogen jet target.

References

- [1] SPIN Collaboration, "Acceleration of polarized protons to 120 GeV and 1 TeV at Fermilab", University of Michigan Report UM-HE 95-09, (1995).
- [2] D.P. Barber, "Prospects for polarized protons at HERA", International School of Nucleon Structure, Erice, Sicily, August 1995; D.P. Barber, "Possibilities for polarized protons at HERA", in Prospects of spin physics at HERA, DESY-Zeuthen, August 1995, DESY Report 95-200; G. Hoffstätter, "Polarized protons in HERA", in Proc. of the DESY Accelerator Group Seminar, DESY Report 96-05, May 1996; V. Balandin, N. Golubeva and D.P. Barber, "Studies of the behaviour of proton spin motion in HERA-p at high energies", DESY Report M-96-04, May 1996.
- P.L. Anthony et al., Phys. Rev. Lett. 71, 959 (1993);
 K. Abe et al., Phys. Rev. Lett. 74, 346 (1995).
- [4] H.E. Jackson, Proc. 11th International Symposium on High Energy Spin Physics, Bloomington 1994, AIP Conf. Proc. **343**, 747 (1995).
- [5] Y. Makdisi, Proc. 11th International Symposium on High Energy Spin Physics, Bloomington 1994, AIP Conf. Proc. 343, 75 (1995).
- [6] J. Feltesse, Proc. of Workshop on Future Physics at HERA (1996).
- [7] SPIN Collaboration "SSC EOI-001" SSC Letter of Intent, 28 November 1990.

2 Hadronic spin physics

The interest in spin phenomena has significantly increased in recent years. It is now clear that spin effects in high energy interactions provide essential information about the elementary particles' properties including: the nucleon wave functions; the short-range and long-range lepton, quark and gluon interactions; chiral symmetry breaking; and confinement. Recently, there has been significant progress in understanding the nucleon's longitudinal spin structure; moreover, new polarization experiments are planned at SLC, HERA and RHIC. The HERA polarized proton beams would allow unique studies of spin phenomena at the highest available energy including: cleaner searches for new particles; direct and unambiguous tests of perturbative quantum chromodynamics (QCD); studies of nonperturbative QCD; and measurements of the transverse spin structure of hadrons.

The HERA accelerated polarized proton beams would allow measurements of one-spin and two-spin asymmetries: in inclusive processes; in elastic scattering; and in hyperon production.

2.1 Physics goals of the SPIN Collaboration

The primary physics goal of the SPIN Collaboration is to study two-spin and one-spin effects in 820 GeV/c proton-proton elastic scattering at large P_{\perp}^2 . We would also study spin effects in inclusive p-p scattering.

Our collaboration would first help to develop an 820 GeV/c spin-polarized proton beam using Siberian snakes to overcome the many depolarizing resonances in DESY's three proton accelerator rings. The 820 GeV/c polarized proton beam would then be scattered from a polarized proton gas jet used as an internal target. The elastic and inclusive events would be detected by a quadrupole-focusing high-luminosity spectrometer about 16 m long. Both the polarized jet and the spectrometer would be quite similar to the devices now being constructed for our NEPTUN-A experiment at the UNK accelerator in Protvino, Russia; this fixed-target elastic and inclusive experiment is scheduled to run with an unpolarized beam at 400 GeV/c when UNK first operates.

Much of the SPIN Collaboration is quite experienced with inclusive and elastic experiments. We made perhaps the world's first inclusive measurement at the ZGS [1] in 1967 by studying $p + p \rightarrow \pi^{\pm} + anything$ at 12 GeV/c. Our group then made the first inclusive measurements at the ISR in 1971 [2] and confirmed Feynman-Yang scaling.

The spectrometer that we propose to use at HERA would be quite similar in concept to the 45 m long inclusive spectrometer used at the ISR [2] and the 55 m long elastic/inclusive spectrometer that will be used at UNK [3].

We also have considerable experience with elastic scattering experiments at high P_{\perp}^2 . We have carried out a number of p-p elastic scattering experiments with unpolarized beams and targets [4, 5]. The break found in the unpolarized $90_{\rm cm}^{\circ}$ p-p elastic experiment at the ZGS [5] in 1966 was perhaps the first experimental evidence for inner structure in the proton; the



same 90° data were later used as the main experimental support for Brodsky's s^{-n} scaling laws of QCD.

Michigan is especially experienced in spin polarization experiments. Using the ZGS polarized proton beam, large and totally unexpected two-spin effects [6] were found in large- P_{\perp}^2 proton-proton elastic scattering. In the hard-scattering region near $P_{\perp}^2 = 5$ (GeV/c)², $d\sigma/dt(\uparrow\uparrow)$ was found to be four times larger than $d\sigma/dt(\uparrow\downarrow)$ as shown in Fig. 2.1 [6]. Concerns by Bethe and Weisskopf, about this being a $90_{\rm cm}^{\circ}$ particle-identity effect rather than a large- P_{\perp}^2 hard-scattering phenomenon, were directly answered by a fixed-angle experiment as shown in Fig. 2.2 [7]. The medium- P_{\perp}^2 points near $P_{\perp}^2 = 2.5$ (GeV/c)², where the spin effects are small, are at $90_{\rm cm}^{\circ}$ just the same as the large- P_{\perp}^2 points near $P_{\perp}^2 = 5$ (GeV/c)², where the spin effects are large; thus it is clearly a hard-scattering phenomenon.

Other members of our Collaboration have been active in polarization experiments at 70 GeV/c at IHEP-Protvino, at 200 GeV/c at Fermilab, at 12 GeV/c at KEK, and at 10 GeV/c at Dubna. We also have a strong group of nuclear experts in spin experiments and accelerator physics, especially from IUCF and TRIUMF.

Figure 2.3. The analyzing power, A, is plotted against P_{\perp}^2 , for spin-polarized proton-proton elastic scattering at 24 and 28 GeV/c [8].

More recently, large and again unexpected high- P_{\perp}^2 spin effects were found in measurements of the one-spin asymmetry A_N in p-p elastic scattering at the AGS [8]. It is quite clear that the once-accepted PQCD prediction, that $A_N = 0$ at high- P_{\perp}^2 and high energy, is not supported by the recent high precision data shown in Fig. 2.3. Because of

the small cross-section, it seems unlikely that one can extend exclusive spin studies much beyond $P_{\perp}^2 = 10 \; (GeV/c)^2$; in fact the largest P_{\perp}^2 exclusive event ever observed [4] was at $P_{\perp}^2 = 15 \; (GeV/c)^2$.

The central physics goal of the SPIN Collaboration is to determine if the large spin effects shown in Figs. 2.1, 2.2 and 2.3 persist at 820 GeV/c.

Figure 2.4. E-704 data of A_N for π production in 200 GeV/c p-p collisions [9].

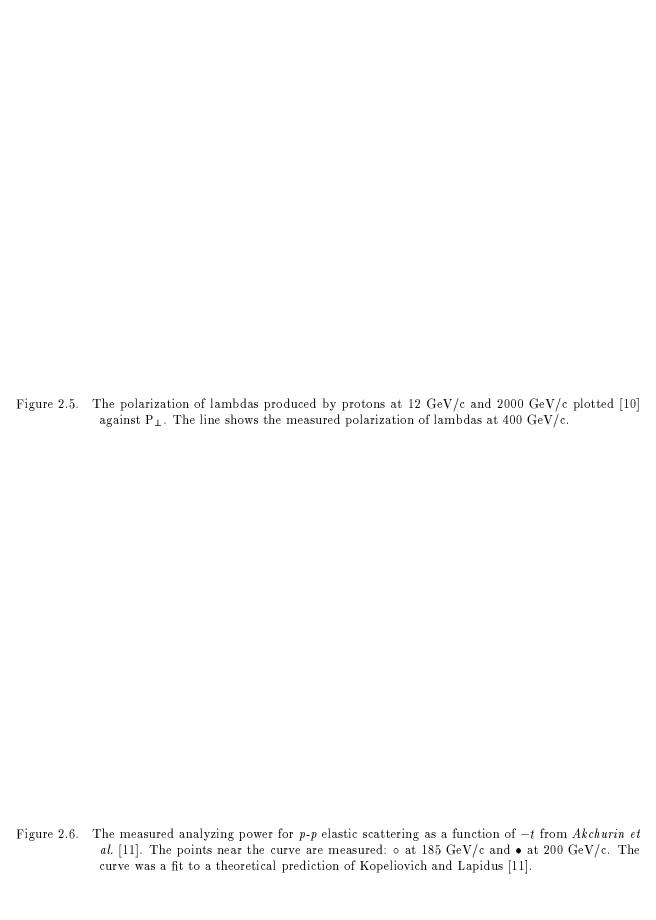
Fig. 2.4 shows the interesting A_N asymmetries observed in the inclusive production of π mesons in 200 GeV/c p-p collisions in E-704 at Fermilab [9].

Fig. 2.5 shows that spin remains very important [10] in inclusive Λ production in proton-proton scattering from 12 GeV/c at KEK, up to 400 GeV/c at Fermilab, and up to about 2 TeV equivalent at the ISR, the world's highest energy proton-proton collider. This evidence indicates that spin is quite important at these high energies.

A great deal of systematics has been found for the polarizations in inclusive hyperon production with strangeness S=1, 2 or 3. However, rather approximate quark rearrangement theoretical descriptions fail to reproduce the full complement of the data. Needed here are selective measurements of one-spin and two-spin observables.

Predictions of "color transparency" suggest that the onset of perturbative QCD may occur at lower energies inside nuclei, because the nucleus preferentially transmits scattered hadrons that have undergone a hard collision. Color screening raises the possibility of using the nucleus as a filter for selective studies of hard scattering contributions to hadron-hadron interactions. If this is indeed true, then one can expect quite different spin-dependent observables for quasi-free scattering compared to free proton-proton scattering.

Fig. 2.6 shows the measured A_N data for p-p elastic scattering as a function of -t at very low $t \simeq 0.001 \text{ (GeV/c)}^2$, and a Coulomb-Nuclear Interference (CNI) fit [11]. By using CNI polarimeters to measure the proton beam polarization, we hope to better measure



the analyzing power and understand the underlying mechanism in the interference between Coulomb and Nuclear amplitudes at very low -t.

In conclusion, there are many spin phenomena that need to be measured at 820 GeV/c including two-spin p-p elastic scattering, and both elastic and inclusive one-spin effects. We believe that precise measurements of spin observables may be necessary to advance our understanding of the strong force at high energy. A spin-polarized 820 GeV/c proton beam could open another dimension at HERA.

References

- [1] L. G. Ratner et al., Phys. Rev. Lett. 18, 1218 (1967).
- [2] L. G. Ratner et al., Phys. Rev. Lett. 27, 68 (1971).
- [3] A. D. Krisch, Experiment NEPTUN-A, in Proc. of Workshop "Physics at UNK", 152 (March 1989), Published by IHEP, Protvino, Ed. A. M. Zaitsev (1989).
- [4] G. Cocconi et al., Phys. Rev. Lett., 11, 499 (1963);Phys. Rev. Lett., 12, 132 (1964).
- [5] C. W. Akerlof et al., Phys. Rev. Lett., 17, 1105 (1966); Phys. Rev. 159, 1138 (1967).
- [6] J. R. O'Fallon et al., Phys. Rev. Lett., 39, 733 (1977);
 D. G. Crabb et al., Phys. Rev. Lett., 41, 1257 (1978).
- [7] E. A. Crosbie et al., Phys. Rev., **D23**, 600 (1981);
 A. Lin et al., Phys. Lett **74B**, 273 (1978).
- [8] D. G. Crabb et al., Phys. Rev. Lett. 65, 3241 (1990);
 - P. R. Cameron *et al.*, Phys. Rev., **D32**, 3070 (1985);
 - D. C. Peaslee et al., Phys. Rev. Lett., 51, 2359 (1983);
 - P. H. Hansen et al., Phys. Rev. Lett., 50, 802 (1983).
- [9] A. Yokosawa, Frontiers of High Energy Spin Physics, eds. T. Hasegawa et al., (University Academy Press Inc., Tokyo 1993) p. 93.
- [10] K. Heller, in Proc. of the 7th International Symposium on High Energy Spin Physics, 1986, IHEP Protvino, 1, 81 (September 1987).
- [11] J. Schwinger, Phys. Rev. 73, 407 (1948); B. Z. Kopeliovich and L. I. Lapidus, Sov. J. Nucl. Phys 19, 114 (1974); N. Akchurin et al., Phys. Lett. B229, 299 (1989), Phys. Rev. D48, 3026 (1993), Phys. Rev. D51, 3944 (1995); D. P. Groznick et al., Nucl. Instrum. Meth. A290, 269 (1990); A. D. Krisch and S. M. Troshin, Estimate of elastic proton-proton polarization at small P²_⊥ near 1 TeV, UM HE 95-20.

3 Elastic 820 GeV/c p-p experiment at HERA

Experiments using an 820 GeV/c polarized proton beam and an internal polarized atomic-hydrogen gas-jet [1] target in the East Hall would allow one to study spin effects in proton-proton collisions in reactions such as:

- elastic scattering at large P_{\perp}^2 (> 3 (GeV/c)²),
- elastic scattering at medium-to-small P_{\perp}^2 ($0.1-3~({\rm GeV/c})^2$),
- elastic scattering at very small P_{\perp}^2 (< 0.1 (GeV/c)²).
- inclusive production of π^{\pm} , π^{0} , K^{\pm} , p^{\pm} and hyperons.

The internal polarized gas jet target and a possible spectrometer for the large P_{\perp}^2 experiments are described below.

3.1 Polarized jet target

One could install Michigan's Mark II ultra-cold proton-spin-polarized atomic-hydrogen gasjet [1] as an internal target in the East Hall; Michigan has been building this target for the NEPTUN-A Experiment at the UNK accelerator in IHEP-Protvino.

The Mark II Jet uses the ultra-cold magnetic method to polarize hydrogen atoms by separating the ultra-cold atoms according to their electron-spin states using a strong magnetic field gradient. As shown in Fig. 3.1, hydrogen molecules are first dissociated into atoms by passing them through an rf dissociator. The hydrogen atoms then cool as they pass through several stages of ever lower temperatures; they finally reach 0.3 K in a stabilization cell, which is the mixing chamber of a He^3 - He^4 dilution refrigerator; the cell walls are coated with superfluid He^4 . In the stabilization cell, the hydrogen atoms encounter a high magnetic field gradient at one end of a 12 T superconducting solenoid. The magnetic field gradient forces atoms in one electron-spin state (low field seekers) out of the cell through a small aperture to form a jet. The field forces atoms of the opposite electron-spin state (high field seekers) behind the cell, where they recombine to form hydrogen molecules on the surfaces.

At the exit of the cell, there is a copper mirror which has a quasi-parabolic shape and is coated with superfluid He^4 . It was shown that, at 0.3 K, the liquid helium reflects the hydrogen atoms due to "quantum reflection" [2]. The mirror shape will be designed to focus the emerging atoms and thus maximize the acceptance in the downstream superconducting sextupole. We saw a factor of 7.5 intensity increase with such a mirror in our prototype jet [3].

An rf transition unit then transfers the electron-spin polarization into proton-spin polarization via the hyperfine transition. Atoms in one proton-spin state are then focused by the superconducting sextupole to form a narrow jet at the interaction region where the jet passes through the accelerator beam. Atoms with the other proton-spin states are defocused by the sextupole.

Finally, at the interaction region, a small holding magnetic field would define the polarization direction of the jet target. Reversing this magnetic field would then reverse the

polarization direction; frequent spin reversals would reduce systematic errors in the experiments.

As shown in Fig. 3.1, a large 2.6 K "catcher", with a measured cryopumping speed of 1.2 10⁷ l s⁻¹, would trap the atoms below the target to keep the nearby ring vacuum at an acceptable level of 10⁻⁹ torr. At the bottom of the catcher, a hydrogen maser polarimeter would measure the polarization of the jet using ring-downs of the maser signals.

We expect to obtain a target thickness at least 10^{13} cm⁻² with a polarization above 90 %. With a beam intensity of $4.4 \cdot 10^{17}$ s⁻¹, the luminosity would typically be $4.4 \cdot 10^{30}$ cm⁻²s⁻¹.

Both the source and the target are expected to improve in intensity with further research and development. The present goal for the source is to exceed 3 mA while the jet goal is about 10^{14} cm⁻². The luminosity would then be about 20 times larger than the above value. One should note that an internal polarized-gas jet could run:

- parasitically with collider experiments;
- without disturbing the circulating beam;
- like a point source without secondary interactions;
- with a high polarization;
- with frequent spin reversals to reduce experimental systematic errors.

Fig. 3.1. Mark II Jet.

3.2 Large- P_{\perp}^2 experiments

It is now known that p-p elastic scattering at large- P_{\perp}^2 has large and unexpected transverse spin effects with either one or both protons polarized. Fig. 3.2 shows a plot [4] of the analyzing power A_N at the incident momenta of 24 and 28 (GeV/c) measured at the AGS and CERN. At the largest measured P_{\perp}^2 of 7 (GeV/c)², the analyzing power was above 20% and appears to be still rising. As discussed in Section 2, perturbative QCD predicted that $A_N = 0$ at large P_{\perp}^2 and high energy, due to helicity conservation in quark and gluon interactions. It would be most interesting to see if this high A_N value persists to 820 GeV/c at HERA.

A three-dimensional compilation of the spin-spin correlation parameter A_{NN} versus P_{\perp}^2 and P_{lab} is shown in Fig. 3.3 [5]. Most of the data up to 13 GeV/c were obtained at the ZGS [6]; a few points at 16.5 and 18.5 GeV/c were obtained at the AGS [5]. Perturbative QCD models predicted that $A_{NN} = 1/3$ for $\theta_{cm} = 90^{\circ}$. The 90°_{cm} curve exhibited a large variation reaching an A_{NN} value of 60% at the highest measured energy of 13 GeV/c. The large P_{\perp}^2 curves also show a rich structure which should be explored at higher energies.

While there is little hope of doing an 820 GeV/c measurement at 90_{cm}° , one could obtain fairly precise data at P_{\perp}^2 values up to about 5 (GeV/c)². For these A_N and A_{NN} measure-

Figure 3.2. Analyzing power at 24 and 28 (GeV/c) [4].

Figure 3.3. A_{NN} vs. P_{beam} and P_{\perp}^{2} [5].

ments, we would use a magnetic spectrometer. Due to the limited space available in the East Hall, we designed a shorter spectrometer by using superconducting magnets instead of warm iron magnets.

3.2.1 Spectrometer

Large- P_{\perp}^2 elastic and inclusive events would be detected using a 16 m long focusing recoil spectrometer that is somewhat similar to the 55-m-long NEPTUN-A spectrometer, which was designed to study 400 GeV proton-proton elastic scattering at UNK in Protvino, Russia. The proposed spectrometer is shown in Fig. 3.4. The quadrupoles Q_1 , Q_2 , Q_3 and Q_4 focus the acceptance of about $\Delta\theta_{lab}=20$ –22 mrad and $\Delta\phi'_{lab}=170$ –180 mrad, so that the detectors and magnet apertures can be rather small. The counters HV1 and HV2 will measure the outgoing horizontal and vertical angles of the recoil particle. The scintillator counters S_1 , S_2 , and S_3 will give a fast first level trigger. The 20° vertical bend down in the M_3 magnets, combined with the 0.5 mm vertical resolution drift wire chambers $W_1 \rightarrow W_4$, would give a momentum resolution of about 0.1%. S_1 and S_2 would also measure the time-of-flight for particle identification at low recoil momentum.

The very precise recoil momentum measurement would strongly discriminate against inelastic and quasi-elastic events. Therefore, one would need only a minimal vertical angle measurement by the forward arm which would probably contain two small vertical resolution hodoscopes and no magnet.

The horizontal and vertical beam envelopes for the spectrometer were obtained using the beam design program TRANSPORT. As shown in Fig. 3.5, these beam envelopes were kept quite small to fit into the small aperture superconducting magnets.

The SPIN collaboration would provide all detectors, logic, and data analysis computers. A complete list of the required magnets is given in Table 3.1. IHEP-Protvino might produce the superconducting dipoles and quadrupoles; it is hoped that DESY could provide their helium and perhaps their power supplies.

Magnet	Length	Diameter	Approximate Position	\mathbf{B}'_{max}	B_{max}
	(cm)	(cm)	Target to center (m)	(T/m)	(T)
Q_1	40	4×8	0.50	128	5.1
$\mathrm{Q}_2,\mathrm{Q}_3,\mathrm{Q}_4$	40	8	1.2, 3.7, 4.3	63	2.5
$\mathrm{M}_{1a},\mathrm{M}_{1b}$	60	8	2.1, 3.0		4.5
${ m M}_2$	60	8	5.0		4.5
$\mathrm{M}_{3a}, \mathrm{M}_{3b}$	60	8	9.6, 10.5		4.5

Table 3.1. Recoil spectrometer magnet list.

3.2.2 Event Rate Estimate

For parasitic running with an internal target, we assume that the circulating polarized (and unpolarized) proton beam intensity at HERA would typically be $I = 4.4 \ 10^{17} \ s^{-1}$ (70 mA



or $9\cdot10^{12}$ stored protons) and with a hydrogen jet target thickness of $T=10^{13}$ cm⁻², the luminosity would then be:

$$\mathcal{L} = I \cdot T = 4.4 \cdot 10^{30} \ cm^{-2} sec^{-1}. \tag{3.1}$$

The SPIN spectrometer acceptance would be $\Delta t \cdot \Delta \phi/2\pi$. Table 3.2 shows the Δt and $\Delta \phi$ acceptances and the interpolated differential p-p elastic cross-section $d\sigma/dt$. We then calculated the event rate for an 820 GeV polarized beam run using the equation:

Rate (Events/day) =
$$\mathcal{L} \cdot \frac{d\sigma}{dt} \cdot \Delta t \cdot \frac{\Delta \phi}{2\pi} \cdot (3600 \ s/hr)(24 \ hr/day)$$
 (3.2)
 = $0.0605 \cdot \frac{d\sigma}{dt} \left(\frac{nb}{(GeV/c)^2}\right) \cdot \Delta t (GeV/c)^2 \cdot \Delta \phi(mrad)$.

These event rates are given in Table 3.2 along with the statistical uncertainty in the analyzing power A_N and the spin-spin correlation parameter A_{NN} .

Table 3.2. Event rates in the spectrometer from Eq. 3.2

		Lubic .	0.2. Lvcii	Tares III o	ne spece	diomicuel ii	Om Eq. 0.2	
P_{\perp}^{2}	Δt	$\Delta \phi$	$d\sigma/dt$	<u>events</u>	days	N	ΔA	ΔA_{NN}
$(\mathrm{GeV/c})^2$	$({\rm GeV/c})^2$	mr	$\frac{nb}{(GeV/c)^2}$	$_{ m day}$		events	$[.95\sqrt{N}]^{-1}$	$[.95(.75)\sqrt{N}]^{-}$
1	0.11	193	2000	2570	20	51300	0.5%	0.6%
2	0.18	213	43	100	60	6000	1.4%	1.8%
3	0.25	232	9	31.5	100	3150	1.9%	2.5%
4	0.33	256	1.5	7.7	200	1530	2.7%	3.6%
5	0.41	273	0.4	2.7	300	812	3.7%	4.9%
6	0.49	289	0.065	0.56	400	223	7.1%	9.4%
7	0.58	312	0.016	0.18				

Clearly the points above $P_{\perp}^2 = 5 \text{ (GeV/c)}^2$ have unacceptably large errors. Later increases in: the target thickness (perhaps $5 \times$ by adding a HERMES type storage cell), the proton beam intensity (perhaps $2 \times$ to 150 mA), and the spectrometer acceptance (perhaps $3 \times$ by later building larger aperture magnets) could increase the event rates by a factor of 30. This factor of 30 would allow fairly precise measurements of the important points at P_{\perp}^2 of 6 and 7 $(\text{GeV/c})^2$; in a 200 day run the errors in A_N would be about $\pm 1.8\%$ at 6 $(\text{GeV/c})^2$ and about $\pm 3.2\%$ at 7 $(\text{GeV/c})^2$. An alternate approach would be a dedicated run where the HERA beam intensity might reach $2 \cdot 10^{14}$ stored protons or 10^{19} protons per sec passing through the target. While this would require some HERA proton beam development, it would allow fairly precise data in dedicated runs of 20-30 days.

3.3 Cost Estimate

A preliminary estimate of the cost for the *p-p* elastic experiment in the East Hall is about **DM 2.5 M**. This includes reconditioning 4 existing superconducting UNK-2 prototype dipoles, fabricating 4 superconducting quadrupoles, and the magnet stands, detectors, drift wire chambers, and the interaction region modifications. The jet target was already funded by the U.S. department of Energy.

References

- [1] V. G. Luppov et al., Proc. SPIN96 Symposium, Amsterdam (1996) to be published.
- [2] J. J. Berkhout et al., Phys. Rev. Lett. 63, 1689 (1989).
- [3] V. G. Luppov et al., Phys. Rev. Lett. 71, 2405 (1993).
- [4] D. G. Crabb et al., Phys. Rev. Lett. 65, 3241 (1990) and references therein.
- [5] D. G. Crabb et al., Phys. Rev. Lett. 60, 2351 (1988);
 - F. Z. Khiari et al., Phys. Rev. **D39**, 45 (1989);
 - A. D. Krisch, Z. Phys. C46, S1533 (1990).
- [6] J. R. O'Fallon et al., Phys. Rev. Lett. 39, 733 (1977);
 - D. G. Crabb et al., Phys. Rev. Lett. 41, 1257 (1978).

4 Theoretical aspects of spin at HERA

In recent years there has been a significant interest in the study of spin phenomena. It is now widely accepted that the physics of spin phenomena in particle interactions provides vital information on the most profound properties of particles: their wave functions, the short and large distance dynamics of the lepton, quark and gluon interactions, and the mechanisms of chiral symmetry breaking and confinement. These systematic spin studies have several well defined goals; some of these include:

- Understand chiral symmetry breaking and helicity non-conservation on the hadronic level.
- Study the overall nucleon structure and long range dynamics.
- Study the nucleon's spin structure, i.e., how the proton's spin state can be obtained from a superposition of Fock states with different numbers of constituents with spin.
- Understand how the dynamics of constituent interactions depend on spin.

The first two goals are related to hadronic long-range (non-perturbative QCD - NPQCD) dynamics, while the last two concentrate on the constituent short-interaction dynamics (perturbative QCD - PQCD). Experiments designed to investigate these important nucleon properties can be performed with a polarized proton beam at HERA. The beam could also be used to test some fundamental assumptions of QCD regarding spin.

4.1 Elastic $pp \rightarrow pp$ scattering

4.1.1 History

Polarized elastic pp scattering experiments were among the first group of spin experiments performed with synchrotrons [1–3]. These experiments raised fundamental questions about spin phenomena, some of which still remain unanswered.

When the differential cross sections for elastic pp were measured at different energies s and momentum transfers -t, they exhibited the unusual behavior that the -t dependence changed over different ranges of the -t variable, but the ranges were relatively independent of s [4–6]. Each range of -t, which exhibits different cross section behavior, defines a kinematic regime where different physical processes are dominant [7]. These three regions are:

- $\bullet\,$ very low P_{\perp}^2 or Coulomb Nuclear Interference (CNI) region,
- moderate P_{\perp}^2 values (0.1 to about 3 GeV²), where there is Pomeron dominance,
- high P_{\perp}^2 , where both the PQCD hard scattering processes and the Landshoff three-gluon exchange processes contribute to the cross sections.

Each region is dominated by a different physics; each could be explored with a polarized proton beam at HERA.

The measurement of the analyzing power (or polarization) A_N at angles far from 90°_{cm} revealed that, contrary to PQCD predictions, A_N was non-zero [8]. The theoretical arguments were based upon the assumption from chiral symmetry that helicity conservation on

the hadronic level was valid. The experimental results imply that this is not true in some kinematic regions. Clearly this is a non-perturbative effect which must be studied further.

The experiments done at the Argonne ZGS and the Brookhaven AGS, which measured the transverse spin asymmetry, A_{NN} , revealed an interesting structure, whose explanation is still a matter of speculation [2, 3, 9]. The PQCD predictions do not hold for any of the energies for which the experiments were performed. A recent analysis by Ramsey and Sivers [10] indicates that there may be some interesting physics in the -t range between 6 and 8 $(\text{GeV/c})^2$. Not only does A_{NN} indicate an onset of structure at 90°_{cm} , but the differential cross section changes its -t behavior at exactly the same range. When the measurements of A_{NN} were done at different angles and energies, similar interesting structure was observed. These same -t values could be explored at HERA energy with a polarized proton beam.

4.1.2 Formalism

We briefly review the formalism of elastic polarized p-p scattering. The kinematics of the $2 \rightarrow 2$ process can be described in terms of the Mandelstam variables s, t, u, while the dynamics can be characterized by the proton wave function and the hard scattering amplitudes, \mathcal{M} , containing the momentum and helicity information for the processes. Using these, we can write the spin observables for elastic pp scattering in terms of the five independent Jacob-Wick helicity amplitudes [11]:

$$\Phi_{1}(s,t) = \langle ++ \mid \mathcal{M} \mid ++ \rangle
\Phi_{2}(s,t) = \langle ++ \mid \mathcal{M} \mid -- \rangle
\Phi_{3}(s,t) = \langle +- \mid \mathcal{M} \mid +- \rangle
\Phi_{4}(s,t) = \langle +- \mid \mathcal{M} \mid -+ \rangle
\Phi_{5}(s,t) = \langle ++ \mid \mathcal{M} \mid +- \rangle.$$
(4.1)

The unpolarized differential cross section is related to these amplitudes by:

$$\frac{d\sigma}{dt} = \frac{\pi}{2s(s-4m^2)} \left[|\Phi_1|^2 + |\Phi_2|^2 + |\Phi_3|^2 + |\Phi_4|^2 + 4|\Phi_5|^2 \right], \tag{4.2}$$

while the other spin observables are written as:

$$\sigma = s(s - 4m^{2}) \frac{d\sigma}{dt}$$

$$A_{N}\sigma = -Im \left[\Phi_{5}^{*}(\Phi_{1} + \Phi_{2} + \Phi_{3} - \Phi_{4}) \right]$$

$$A_{NN}\sigma = Re \left[\Phi_{1}\Phi_{2}^{*} - \Phi_{3}\Phi_{4}^{*} + 2 \mid \Phi_{5} \mid^{2} \right]$$

$$A_{SS}\sigma = Re \left[\Phi_{1}\Phi_{2}^{*} + \Phi_{3}\Phi_{4}^{*} \right]$$

$$A_{LL}\sigma = \frac{1}{2} \left[- \mid \Phi_{1} \mid^{2} - \mid \Phi_{2} \mid^{2} + \mid \Phi_{3} \mid^{2} + \mid \Phi_{4} \mid^{2} \right].$$
(4.3)

Here the directions of spin are L for the longitudinal component (with respect to the proton momentum) while the transverse components are N (normal) and S (sideways) respectively.

It is assumed that the soft (Regge) and hard contributions can be separated out in each kinematic region.

The quantities Φ_5 and Φ_2 are the single and double spin-flip amplitudes, respectively. The observables which are sensitive to these amplitudes, such as the polarization A_N , are measures of the degree of hadronic helicity non-conservation. The other observables measure which amplitudes dominate in each kinematic region and give indications of the spin properties of hadronic structure. This could indirectly shed light on unknown properties of the proton wave function, such as its kinematic properties and its overall normalization.

4.1.3 Phenomenology

The kinematic regime of the proposed pp elastic experiments at HERA falls in the "hard scattering" region, i.e., $m_p^2 \ll |t| \ll s$. In this region, the t-dependent Landshoff amplitudes have a significant contribution to the spin observables. Physically, these correspond to independent valence quark scatterings, which have a finite effective impact parameter. In contrast, the pointlike contributions of the Quark Interchange Model (QIM) have different s and t dependencies. One could investigate the relative contributions of these processes by measuring the spin observables over the full range of -t available at HERA. This should give insight into the physics of helicity conservation and hadronic structure.

In the traditional Regge theory approach, the polarization (A_N) vanishes in the large s limit. The hard scattering approach, however, allows for helicity flip effects associated with the hadronic wave function. If we assume that we can structure the proton wave function from scattered quarks which are approximately collinear, then the corresponding parameterization of Φ_5 allows us to test our QCD-motivated assumptions about the spin properties of the wave function. In particular, this model [10] predicts that, at HERA energies, the polarization should behave as follows:

- at small -t there is an overall $(-t)^{\frac{1}{2}}$ dependence and A_N should decrease with energy, indicative of its coherent Regge behavior, and
- at large -t the polarization becomes asymptotically energy independent and should behave like $(-t)^{-\frac{1}{2}}$ at large s.

Existing polarization measurements [1, 2, 8] are consistent with these predictions, but the kinematic data range is limited. The proposed experiments at HERA would greatly expand the range of this data.

Since the QIM and Landshoff contributions to the amplitudes have different kinematic dependencies, testing predictions for the other spin observables [10] for fixed angle and separately for fixed -t, would yield significant information regarding the form of the proton wave function at these energies. It might also provide insight on possible non-perturbative contributions to elastic hadron scattering. Currently, such contributions can be accounted for only by various model approaches which were reviewed in [12].

4.2 Inclusive polarized pp interactions

4.2.1 History

Studies of inclusive particle production in $p + p_{\uparrow}$ (single spin) and $p_{\uparrow} + p_{\uparrow}$ (double spin) interactions could give valuable information on:

- the nature of parton subprocesses,
- parton spin distributions and non-perturbative effects such as the orbital angular motion of the proton constituents.

Experimental studies of polarized inclusive production above 100 GeV/c began in the late eighties at Fermilab, where the E-704 collaboration measured single spin asymmetries in pion production at various values of transverse momenta. In the CNI region of $|t| \le 0.05$ [13], the data agree with the expected interference between amplitudes, but the overall kinematic range was limited and the error bars were large because of the low intensity of the hyperon-decay polarized proton beam. The mid-t region data [13] revealed surprising results regarding:

- the existence of large polarizations in pion production,
- the kinematic dependence of the asymmetries.

Single spin asymmetries for high transverse momenta were measured for π^0 production [14]; these showed a polarization mostly consistent with zero from $1.0 \le |t| \le 4.0 \text{ (GeV/c)}^2$. Various theoretical models were proposed to describe the data. However, more precise single spin measurements for $p + p_{\uparrow} \to \pi + anything$ in a wider kinematic range are needed to distinguish between these models. The proposed polarized proton experiments at HERA would provide precise data over a larger kinematic range than E-704, since:

- the luminosity would be higher,
- the polarization would be higher,
- the energy would be higher.

These HERA experiments would certainly enhance the available data and should increase our understanding of the underlying physics.

The two-spin asymmetries in pion production for $p_{\uparrow} + p_{\uparrow} \rightarrow \pi^{\pm} + anything$ were also measured in E-704 at Fermilab [15], but the error bars were large. The A_{LL} data are consistent with zero for $1 \leq P_{\perp} \leq 3 \text{ GeV/c}$. For these two-spin inclusive experiments, the kinematic range could be greatly expanded at HERA and much better precision could be attained.

4.2.2 Phenomenology

Since the single spin asymmetries for pion production are not well understood, we will summarize some of the present theoretical models which try to explain the existing data.

The mid-t data can be explained by an orbiting valence quark model developed by T. Meng $et\ al.$ [16]. The non-zero asymmetry can be attributed to the orbital motion of the valence quarks in a transversely polarized proton. This is a non-perturbative effect which must be tested by experiment. This model can also be extended to kaon production [17]. More precise measurements of A_N for a large range of -t and x_F values would test this model and indirectly measure the proton's orbital angular momentum.

Reference [18] argued that the orbital motion of quark matter inside a constituent quark is the origin of the observed asymmetries in inclusive pion production at moderate and high transverse momenta. This non-perturbative mechanism predicts significant asymmetries at P_{\perp} near 1 GeV, where the internal structure of a constituent quark can be probed.

X. Artru has proposed a string model to explain these same asymmetries [19] which gives the proper signs. A third model explains the data in terms of quark interactions with the QCD vacuum field instantons [20]. These interactions lead to an asymmetry in the space and transverse momentum dependence of the proton wave function, which manifests itself in the measured asymmetries of pion production. Clearly, more precise data are needed over a wider kinematic range to distinguish between these theoretical models.

The double spin asymmetries have been predicted for pion production, direct photon production and jet production, based on a QCD hard-scattering model [21]. Since one of the subprocesses in meson production from $p_{\uparrow} + p_{\uparrow}$ scattering involves the qG vertex, these process could be sensitive to the polarized gluon density if it is large. Measuring A_{LL} in $p_{\uparrow} + p_{\uparrow} \rightarrow \pi^0 + anything$ for various P_{\perp} would indicate the relative size of the polarized gluon distribution. The two-spin process cross section for $p_{\uparrow} + \bar{p}_{\uparrow} \rightarrow \pi^0 + anything$ should also be measured. Gluonic effects cancel in the differences of the asymmetries for pp versus $p\bar{p}$; thus the data would directly measure the polarized valence quark distributions in the proton. These distributions become important in the crucial tests of the Bjorken Sum Rule, which is a fundamental assumption of QCD.

4.3 Deep inelastic ep scattering

4.3.1 History

Spin structure studies mainly involve inclusive processes such as the deep inelastic scattering of leptons on nucleons. Historically, the deep inelastic scattering of electrons first proved the existence of point-like constituents in the nucleon. The first spin structure measurements of the proton were performed in the 1970's when the SLAC-Yale collaboration measured the spin structure function $g_1(x)$. In the late 1980's, the unexpected EMC results obtained at CERN triggered great theoretical activity [22]. Currently, much attention is focused on the physics of polarized lepton-hadron interactions, largely due to the recent data on polarized inclusive and semi-inclusive deep-inelastic scattering. The data obtained at SLAC and CERN [23] has already implied several conclusions about the nucleon spin structure in the kinematic region of $Q^2 \simeq 2 \to 10 \; (\text{GeV/c})^2$ and Bjorken $x \simeq 0.003 \to 0.7$. The analysis of these data in the framework of perturbative QCD has provided information on the longitudinal polarized parton distributions $\Delta q_i(x,Q^2)$, which are interpreted as the difference of the probabilities $q_i^{+/-}(x,Q^2)$ for finding partons of the flavor i with their spin parallel (+) or antiparallel (-) to the parent nucleon's spin. The results have caused modifications of the earlier quark models of the nucleon's spin and have created other controversies regarding the amount of spin carried by the strange sea quarks and the gluons [24]. Thus, although there has been significant progress in understanding the nucleons' spin structure, present data have left unanswered questions regarding the:

- detailed spin structure of the nucleons,
- relations between polarized and unpolarized quark and gluon structure functions,
- factorization of the quark distributions and its relation to the gluon anomaly [25].

4.3.2 Formalism

Let us briefly review the formalism of deep inelastic polarized electron scattering on a polarized proton. In this case the hadronic tensor $W_{\mu\nu}$ depends on the momenta p and q and on the covariant pseudovector of the proton spin s.

Taking into account translation invariance, the hadronic tensor can be rewritten as a Fourier transformation of the matrix element of the commutator of two currents:

$$W_{\mu\nu}(p,q,s) = \frac{1}{2\pi} \int d^4\xi e^{iq\xi} \langle p, s | [J_{\mu}(\xi), J_{\nu}(0)] | p, s \rangle = W_{\mu\nu}^{[S]} + iW_{\mu\nu}^{[A]}, \tag{4.4}$$

where $|p,s\rangle$ denotes the proton state with momentum p and spin s.

The functions $W_{\mu\nu}^{[S]}$ and $W_{\mu\nu}^{[A]}$ are determined by the discontinuity of the symmetric and antisymmetric parts of the forward Compton scattering amplitude:

$$W_{\mu\nu}^{[S,A]} = \frac{1}{\pi} \text{Im} T_{\mu\nu}^{[S,A]}.$$
 (4.5)

The two spin structure functions G_1 and G_2 enter the expression for the antisymmetric part of the hadronic tensor $W_{\mu\nu}^{[A]}(p,q,s)$:

$$W_{\mu\nu}^{[A]} = \frac{1}{M} \varepsilon_{\mu\nu\lambda\sigma} q^{\lambda} [M^2 s^{\sigma} G_1(\nu, Q^2) + (p \cdot q s^{\sigma} - s \cdot q p^{\sigma}) G_2(\nu, Q^2)]. \tag{4.6}$$

This relation provides the opportunity to apply the helicity amplitude formalism which is especially useful in the case of targets with spins greater than $\frac{1}{2}$. For a spin- $\frac{1}{2}$ target there are only four independent helicity amplitudes in forward Compton scattering and hence four independent structure functions. The spin-dependent structure functions G_1 and G_2 determine the asymmetries which depend on the initial state lepton and nucleon polarizations. In the Bjorken limit (ν and $Q^2 \to \infty$, $x \to \text{constant}$), scaling is valid and the functions G_1 and G_2 should depend only on x, up to the logarithmic corrections, i.e. they should obey the relations:

$$M^2 \nu G_1(\nu, Q^2) \rightarrow g_1(x),$$

 $M \nu^2 G_2(\nu, Q^2) \rightarrow g_2(x).$ (4.7)

Studies of deep inelastic scattering processes in the Bjorken limit provide knowledge on the spin structure of the hadronic constituents.

Operators of twist-two correspond to the vector and axial vector currents for the process of the virtual Compton scattering which determine the hadronic tensor $W_{\mu\nu}$. Twist-two operators provide the finite contribution to the structure functions in the deep inelastic limit while the contribution of twist-three operators are suppressed by a factor of M/Q. Transverse spin structure functions, for example, are of the twist-three type.

4.3.3 Phenomenology

It can be shown that the first moment of the proton structure function $g_1^p(x, Q^2)$ is determined by the following:

$$\int_0^\infty dx \ g_1^p(x,Q^2) \ = \ \frac{1}{2} \left[\frac{4}{9} \Delta u(Q^2) + \frac{1}{9} \Delta d(Q^2) + \frac{1}{9} \Delta s(Q^2) \right] \times$$

$$\left(1 - \frac{\alpha_s(Q^2)}{\pi} + O(\alpha_s^2)\right) + O\left(\frac{\Lambda^2}{Q^2}\right), \tag{4.8}$$

where

$$\Delta q(\mu^2) s_{\nu} = \langle p, s | (\bar{q} \gamma_{\nu} \gamma_5 q) |_{\mu^2} | p, s \rangle. \tag{4.9}$$

In Eq. 4.9, μ^2 is the relevant mass scale or the renormalization point for the axial-vector current operator. The functions $\Delta q(Q^2) \equiv q^+(Q^2) - q^-(Q^2)$ are related to $\Delta q(\mu^2)$ by the QCD evolution equations.

To determine the relative contributions of the quark flavors to the proton spin, one can use the Bjorken sum rule and hyperon decay information along with the experimental data on g_1^p . Briefly summarizing reference [25], the Bjorken sum rule relates the first moment of the difference between the proton and neutron structure functions, $g_1^p - g_1^n$, to nucleon beta decay:

$$\int_0^1 [g_1^p(x) - g_1^n(x)] dx = \frac{1}{6} g_A (1 - \frac{\alpha_s(Q^2)}{\pi} + h.o.c.), \tag{4.10}$$

where g_A is measured in nucleon beta decay and h.o.c. refer to calculated higher-order QCD corrections. Under the assumption of exact $SU(3)_f$ -symmetry the other non-singlet combination, $\Delta u + \Delta d - 2\Delta s$, obeys the equation:

$$\Delta u + \Delta d - 2\Delta s = 3F - D,\tag{4.11}$$

where the parameters F and D can be extracted from the data on semi-leptonic decays of hyperons. The above two equations along with data on g_1 allow a simple determination of the three unknown quantities Δu , Δd and Δs .

A crucial problem here is extrapolation of $g_1(x)$ to x=0. This region of small x provides insight into the interface between the perturbative and non-perturbative regions of QCD. The small-x behavior of the structure function $g_1(x)$ has been described traditionally in the Regge model by the contribution of the a_1 trajectory with intercept $\alpha_{a_1}(0) \simeq 0$. Theoretical justification for the Regge extrapolation is questionable, since it deals with the amplitudes of virtual external particles. In fact, the SMC data imply that $g_1(x)$ might increase at small x. Indeed perturbative QCD evolution gives another form for g_1 at small x, i.e. $g_1(x) \sim \exp \sqrt{\ln 1/x}$. Other forms of this dependence are allowed in Regge formalism with the interpretation of the two-gluon model for the Pomeron. Even such a strong growth as $g_1 \sim \ln^2 x/x$ is possible; then the first moment of g_1 is divergent. An important question here is the role of unitarity for the amplitudes with virtual external particles, i.e. does unitarity restrict the growth of g_1 ? Thus the problem of extrapolation to x=0 is fundamentally important in understanding the proton structure at small x.

Resolving this problem requires experimental measurements of g_1^p in the x region of $10^{-4} - 10^{-5}$ at HERA. In addition, a polarized proton beam at HERA could solve a number of other important problems, such as:

- the role of higher twist processes,
- tests of fundamental assumptions of QCD, such as the Bjorken Sum Rule.

The above discussions focus on deep inelastic scattering from polarized protons and its relation to the structure function $g_1(x, Q^2)$, which is related to the longitudinal polarization

of the proton spin. In the parton model, g_1 effectively measures the quark helicity density. The second spin-dependent proton structure function $g_2(x, Q^2)$ is related to transverse polarization of the nucleon spin and gets contributions from both twist-two and twist-three operators simultaneously. It has been measured at SLAC (E143) in a limited x region. A few theoretical results have been obtained for the function $g_2(x)$, but a simple partonic interpretation is only possible for the twist-two operator contribution. The twist-three contributions are not well understood. The following relation exists between the functions g_1 and g_2 :

$$g_2(x,Q^2) = \int_x^1 \frac{dy}{y} g_1(y,Q^2) - g_1(x,Q^2). \tag{4.12}$$

The above relation is used to calculate $g_2(x, Q^2)$ from $g_1(x', Q^2)$ at $x' \geq x$ in the framework of the parton model with free on–shell partons. However there are no reasons to neglect the contributions of twist-three operators at low enough Q^2 and therefore g_2 can be represented as follows:

$$g_2(x, Q^2) = g_2(x, Q^2)^{[2]} + g_2(x, Q^2)^{[3]},$$
 (4.13)

where the first term on the right hand side of Eq. 4.13 is provided by Eq. 4.12. The twist-three operator contributions $g_2(x,Q^2)^{[3]}$ depend on the effects of quark-gluon interactions and quark masses. In particular, the case of massive off-shell quarks has been studied in the framework of the covariant parton model.

Experimental measurements of $g_2(x, Q^2)$ provide a direct way to study the magnitude of twist-3 contributions and accurate data obtained at HERA with polarized proton beams would be crucial in determining the magnitude of these contributions. Data could also provide a test for the Burkhardt-Cottingham sum rule:

$$\int_0^1 g_2(x) = 0. (4.14)$$

The success or failure of Eq. 4.14 depends on its long-range behavior which, in the simple models, is such that this sum rule is satisfied in perturbative QCD. Thus, valuable information regarding both perturbative and non-perturbative processes could be obtained with polarized protons at HERA.

4.4 Conclusion

In addition to the above-mentioned polarization experiments on:

- p-p elastic scattering,
- p-p inclusive production,
- e-p deep inelastic scattering,

there are many other possible polarization experiments that could be done with polarized protons at HERA. These experiments include:

- semi-inclusive measurements of hadronic final states, such as diffractive Λ production, could study a proton's polarized strange sea distribution.
- jets, open charm, and hidden charm production measurements could study the polarized gluon contribution to the nucleon spin, ΔG .

• tests of the Standard Model, including precise measurements of $\sin^2 \theta_W$.

As pointed out in this short review, there are many important questions which could be addressed by accelerating a polarized proton beam to 820 GeV/c at HERA. This facility could provide fairly high luminosity, high polarization and a great range of energy and transverse momentum. It would allow crucial tests of QCD and studies of the nucleon's spin structure and its interactions; the physics motivation for this program seems quite solid.

References

- [1] G.W. Abshire et al., Phys. Rev. Lett. 32, 1261 (1974).
- [2] J.R. O'Fallon et al., Phys. Rev. Lett. 39, 733 (1977); D.G. Crabb et al., Phys. Rev. Lett. 41, 1257 (1978).
- [3] A. Lin et al., Phys. Lett. **74B**, 273 (1978); E.A. Crosbie et al., Phys. Rev. **D23**, 600 (1981).
- [4] C.W. Akerlof et al., Phys. Rev. 159, 1138 (1967); R.C. Kammerud et al., Phys. Rev. D4, 1309 (1971).
- [5] M.J. Alguard et al., Phys. Rev. Lett. 37, 1261 (1976); G. Baum et al., Phys. Rev. Lett. 51, 1135 (1983).
- [6] A. Bohm et al., Phys. Lett. 49B, 491 (1974); E. Nagy et al., Nucl. Phys. B150, 221 (1979); K.J. Foley et al., Phys. Rev. Lett. 15, 45 (1965).
- A. Donnachie and P.V. Landshoff, Z. Phys. C2, 55 (1979); Phys. Lett. 123B, 345 (1983); Nucl. Phys. B231, 189 (1983); B244, 322 (1984); B267, 690 (1986).
- [8] D.G. Crabb et al., Phys. Rev. Lett. 65, 3241 (1990).
- [9] F.Z. Khiari et al., Phys. Rev. **D39**, 45 (1989); D.G. Crabb et al., Phys. Rev. Lett. **60**, 2351 (1988).
- [10] G.P. Ramsey and D. Sivers, Phys. Rev. **D52**, 116 (1995); Phys. Rev. **D45**, 79 (1992); Phys. Rev. **D47**, 93 (1993).
- [11] M. Jacob and G.C. Wick, Ann. Phys. 7, 404 (1959).
- [12] S. M. Troshin and N. E. Tyurin, Spin Phenomena in Particle Interactions, World Scientific, 1994.
- [13] N. Akchurin et al., Phys. Lett. B229, 299 (1989); Phys. Rev. D48, 3026 (1993);
 D.L. Adams et al., Z. Phys. C56, 181 (1992); Phys. Lett. B261, 197 (1991); Phys. Lett. B264, 462 (1991).
- [14] D.L. Adams et al., Phys. Lett. **B276**, 531 (1992).
- [15] D.L. Adams et al., Phys. Lett. **B261**, 197 (1991).
- [16] T. Meng et al., Phys. Rev. **D49**, 3759 (1994); Phys. Rev. **D51**, 4698 (1995); Phys. Rev. **D52**, 529 (1995).
- [17] T. Meng, Proceedings of the "Workshop on the Prospects of SPIN PHYSICS at HERA", Zeuthen, eds. J. Blümlein and W.-D. Nowak, 1995.
- [18] S. M. Troshin and N. E. Tyurin, Phys. Rev. **D52**, 3862 (1995).
- [19] X. Artru, Proceedings of the "V Workshop on High Energy Spin Physics", Protvino, 1993.
- [20] N.I. Kochelev and M. Tokarev, preprint IFUP-TH 50/92.
- [21] G.P. Ramsey and D. Sivers, Phys. Rev. **D43**, 2861 (1991).
- [22] J. Ashman et al., Phys. Lett. **B206**, 364 (1988); Nucl. Phys. **B328**, 1 (1989).
- [23] D.L. Adams et al., Phys. Lett. B329, 399 (1994); Phys. Lett. B357, 248 (1994); P.L. Anthony et al., Phys. Rev. Lett. 71, 959 (1993); K. Abe et al., Phys. Rev. Lett. 74, 346 (1995).
- [24] M. Goshtasbpour and G.P. Ramsey, hep-ph/9512250.
- [25] C. Bourrely et al., hep-ph/9604204; C. Bourrely and J. Soffer, Phys. Rev. **D53**, 4067 (1996).

5 High intensity polarized H⁻ source

The ideal requirements for the polarized H⁻ source for DESY are a 20 mA current in 100 μ sec pulses at 0.25 Hz within a normalized emittance of 2π mm·mrad for 90% of the beam, with a polarization of 80%. This level of performance has yet to be demonstrated, but it may be attainable using proven technology with an optically-pumped polarized-H⁻ ion source (OPPIS). The OPPIS is one of two competing H⁻ source technologies; the other is the atomic beam source (ABS). The intensity requirement may be reduced if a stacking scheme is used; but then a 3 Hz frequency may be necessary.

The characteristics of the two competing H⁻ source technologies were described in the SPIN Collaboration's Report to Fermilab [1]. Both types of sources have shown recent remarkable increases in current, spurred on by the competition to provide more than 1 mA of pulsed current. At present, the dc OPPIS has produced currents of 1.6 mA, and the pulsed ABS has peak currents up to 1.0 mA. The ABS has the potential for further significant gains to about 5 mA H⁻ peak current over the short term and possibly higher in the future, as discussed in Section 5.2; achieving a current of 20 mA seems optimistic within the near future. The OPPIS development described in Section 5.1 has considerable room for further increases in current if it is pulsed, as expected from broad theoretical considerations and supported by recent experimental results [2]. Further R&D on both ABS and OPPIS sources should be supported.

5.1 Pulsed OPPIS with atomic hydrogen injector

The first stage of the present dc OPPIS consists of an Electron Cyclotron Resonance (ECR) proton source situated in the same high solenoidal magnetic field as an optically pumped rubidium vapor cell. (A 2.5 T magnetic field preserves the electronic polarization of the excited hydrogen atom – formed by a fast proton picking up a polarized Rb valence electron – as it decays to the ground state). The present source current is limited by the large emittance of the ECR proton source and by the approaching space charge limit on the proton current density at the small ECR extraction apertures.

The proposed pulsed source avoids the ECR proton source and its shortcomings by injecting axially a very intense pulsed, high brightness atomic hydrogen beam into the solenoidal field. The hydrogen atoms are then ionized with 80% efficiency in a pulsed-gas He cell to form a small emittance, intense proton beam within the solenoidal field. In the original version [3], the He cell is biased to separate (in energy) atomic hydrogen and protons. The proton beam is then incident on the Rb vapor in exactly the same way as in the dc source. More efficient versions would take advantage of the very high power obtainable from pulsed lasers to optically pump relatively thick Rb vapor targets, allowing one also to take advantage of spin exchange between atomic hydrogen and polarized Rb. In that case the atomic hydrogen leaving the He cell can also be polarized by the Rb and it is not necessary to bias the He cell. The current would then increase because all the beam is used and the beam optics are improved.

Figure 5.1. Proposed pulsed OPPIS: (1) plasmatron proton source; (2) H₂ neutralizer; (3) superconducting solenoid; (4) He ionizer; (5) polarized Rb neutralizer; (6) deflection plates; (7) Na negative ionizer; (8) bending magnet; (9) RFQ.

We hope to obtain 20 mA of polarized H⁻ current from a pulsed OPPIS, using the existing TRIUMF dc OPPIS as a test stand and pulsed technology developed at the Budker Institute of Nuclear Physics (BINP) and at the Institute of Nuclear Research (INR), Moscow.

Figure 5.1 is a schematic of the proposed pulsed OPPIS for DESY. The BINP atomic hydrogen injector consists of a plasmatron proton source, a solenoid for focusing the proton beam, and a pulsed-gas H_2 cell for neutralizing the proton beam. All these components are outside the high solenoidal field containing the Rb vapor cell. As stated above, the neutralized hydrogen beam is then injected into the He cell, which effectively serves as a proton source within the high magnetic field.

The plasmatron discharge produces a point-like plasma emitter having a density of about 10^{15} cm⁻³ and an electron temperature of about 5 eV. The plasma expands freely into the surrounding vacuum and its temperature drops rapidly. The proton extraction electrodes are placed far enough away from the plasma source to take advantage of the cooling and thus produce a bright, small emittance beam of protons. The central 4 cm diameter of the plasma stream is used for production of the brightest 3 A beams. The proton beam is focused by a solenoid that produces a converging beam, which is then immediately neutralized.

At the end of the existing TRIUMF OPPIS is a Na vapor cell that negatively ionizes nuclear polarized H⁰ to form the final H⁻ beam. Its aperture is 2 cm in diameter, in order to keep the H⁻ beam within an emittance of 2 π mm·mrad. In experiments at BINP with an atomic hydrogen injector, the pulsed OPPIS geometry was closely reproduced. An atomic

hydrogen flux of 360 mA equivalent was transmitted through the simulated 2 cm aperture Na ionizer. Assuming 80% conversion to protons in a He cell, 80% conversion to polarized atomic hydrogen in Rb, and 9% H $^-$ yield in the Na cell gives an estimated current of more than 20 mA polarized H $^-$ in a real source. Here it is interesting to note that the same source running unpolarized H $^-$ beam would produce more than 30 mA within an emittance of less than 0.5 π mm·mrad. This is because the He ionizer and polarized Rb neutralizer stages would not be required, and the H $^-$ yield would be 9% of 360 mA. The emittance would be very small in this case because no polarization-preserving 0.14 T magnetic field would be required at the Na cell.

We have constructed parts for an atomic hydrogen injector in collaboration with BINP and INR Moscow, and wish to test our ideas on the operational TRIUMF OPPIS between experimental runs. We also constructed a tunable, pulsed Ti:sapphire laser at TRIUMF using a flashlamp-pumped rod from KEK, and used it to show that one can produce 100% polarized Rb, in conditions suitable for a pulsed 20 mA OPPIS, in 100 μ sec pulses. Although the peak laser power was about 1 kW, 30 to 40 W is sufficient [4], at least in the biased-Hecell version of the pulsed OPPIS. The laser pulse duration depends mainly on the flashlamp pumping duration, and it is a simple matter to increase both if required, without sacrificing polarization.

The beam energy inside the source is 3 keV. The source is relatively compact (slightly over 2 m in length) and can be biased to provide higher energy beams. Figure 5.1 shows the source arbitrarily configured for 20 keV beam energy. The acceleration occurs immediately downstream of the Na negative ionizer, thus minimizing the effects of space charge on the 3 keV H⁻ beam. The beam then enters a bending magnet that sends it either to an RFQ, or to a low energy polarimeter. The bending angle is chosen to preserve the longitudinal polarization of the beam. Optical pumping and diagnostic laser beams pass down the axis of the source. The source is shown built with a superconducting solenoid, as in the dc TRIUMF source, but for pulsed operation at up to 1 Hz a conventional pulsed solenoid would be cheaper and just as effective.

5.2 Atomic beam source with resonant charge-exchange plasma ionizer

A state-of-the-art pulsed ABS (Fig. 5.2) developed by A. Belov et al. [5] at INR Moscow incorporates pulsed H_2 gas fed into an $H_2 \rightarrow 2H^0$ dissociator with pulsed rf power feed and a cold (30 – 80 K) H^0 atomic beam forming nozzle. Gas pulsing significantly reduces ambient gas pressures in subsequent ABS stages, thereby reducing gas scattering losses and increasing atomic beam flux into the ionizer. The reduced average velocity and velocity spread of the cold beam also increases the efficiency of the electron-spin selection (Stern-Gerlach) multipole magnets for focusing the atomic beam into the ionizer volume, and the lower velocity also increases ionization efficiency. The polarized H^0 fluxes into the ionizer approach $1-2 \times 10^{17}$ atoms/sec.

Pulsed beams of polarized H⁻ ions are produced from the polarized H⁰ beam by charge-exchange reaction with D⁻ ions in a dense deuterium plasma injected into the ionizer region from a high-current, pulsed D⁻ plasma source. Peak pulse H⁻ currents of 1 mA have been extracted from such a charge-exchange plasma ionizer over a pulse length of 100 μ s with

Figure 5.2. Schematic of the present INR Moscow atomic beam source with D⁻ resonant charge-exchange ionizer for polarized H⁻ production.

87% polarization (or 90% for pulses of shorter duration) and a normalized emittance of 2π mm mrad.

Further increases in D⁻ density in the deuterium plasma by a factor of about two can be realistically expected with further improvements of the plasma converter, which in turn should yield further proportional increases in polarized H⁻ intensity for the ABS with a resonant charge-exchange plasma ionizer because no saturation with increasing D⁻ current has yet been observed. Ultimately, stripping of H⁻, by plasma electrons and the recombination of H⁻ with plasma D⁺ ions, will limit the maximum useful plasma density, but this is estimated to occur at plasma densities around 10¹¹ cm⁻³, corresponding to H⁻ output currents of about 10 mA at present H⁰ densities in the ionizer.

An additional significant increase in H⁻ intensity would also be realized from an increase in H⁰ atomic beam flux into the plasma charge-exchange region. At present, the useable acceptance volume of the ionizer is about three times larger than the region filled by the H⁰ beam from the ABS. A new, larger-acceptance atomic beam focusing system matched to the ionizer acceptance would entail replacing the conventional, small-bore (3 cm aperture) sextupole magnet system with a combination of 4 T pole-tip field, 8 cm aperture supercon-

ducting sextupoles. The optimum geometry of these high-field sextupoles has been calculated at INR using a Monte-Carlo atomic beam transport simulation code.

The calculated factor of 2.5 improvement in H^0 flux into the ionizer due to use of superconducting sextupoles, combined with a possible factor of 2 increase in the D^- plasma density in the ABS ionizer, should yield an H^- peak current of about 5 mA into 2 π mm mrad normalized emittance with 90% polarization. This factor of 5 increase in H^- yield involves well-understood and available technology and could be implemented in the INR Moscow source within 6 months if requisite funds were made available.

A possible further increase in H⁻ intensity could in principle be provided by using storage of polarized hydrogen atoms in the charge-exchange region of the plasma ionizer. During the past few years the storage cell technique has been developed (for polarized internal gas target application in storage rings) to the point where polarized hydrogen atom target thicknesses of 10^{14} cm⁻² have been obtained by the HERMES group for continuous mode ABS operation. For pulsed operation a factor of two gain in atomic beam intensity should provide a peak target thickness of 2×10^{14} cm⁻² even for an ABS with standard electromagnetic sextupoles. If a deuterium plasma jet is passed through the interaction region, one expects almost total conversion of D⁻ ions into polarized H⁻ in the target because of the very large cross section for resonant charge-exchange of 10^{-14} cm². This method could thus lead to production of polarized H⁻ beams in the future with intensity close to the intensity of unpolarized D⁻ ions which can be transmitted through the ionizer solenoid. At this time, 10 mA of D⁻ current has been transmitted through the ionizer solenoid and extracted from the ionizer on the INR test-bench.

Several problems could arise to limit the use of the storage cell technique for production of intense polarized H⁻ beams by resonant charge-exchange, such as changes of storage cell wall properties as a consequence of intense deuterium plasma bombardment, as well as various depolarization mechanisms. Studies of these effects are planned to be undertaken at INR Moscow starting at the end of this summer.

5.3 Cost Estimate

We estimate that the high intensity polarized ion source would cost about **DM 2.7 M**. The construction time could be approximately 1.5 years.

References

- [1] SPIN Collaboration, "Acceleration of polarized protons to 120 GeV and 1 TeV at Fermilab", University of Michigan Report UM-HE 95-09 (1995).
- [2] A.N. Zelenski et al., Proc. 6th Int. Conf. on Ion Sources (Whistler); Rev. Sci. Instrum. 67, 1359 (1996).
- [3] A.N. Zelenski et al., Nucl. Instrum. Meth. A245, 223 (1986).
- [4] C.D.P. Levy et al., Proc. Int. Workshop on Polarized Beams and Polarized Gas Targets (Cologne), 1995, World Scientific, page 120.
- [5] A. Belov et al., Proc. 6th Int. Conf. on Ion Sources (Whistler); Rev. Sci. Instrum. 67, 1293 (1996).

6 Low energy polarized beam hardware

6.1 General layout

The polarized H⁻ source will need considerably more area than is currently available in the present ion source room. The physical body of the ion source and a new RFQ could be installed in place of the existing magnetron source RFQ. The distance from the source to the RFQ should be minimized in order to ensure high transmission efficiency. An OPPIS source requires about 2 m by 3 m for the source footprint, about 2 m by 4 m for the power supplies and a small console, and 1.5 m by 2.5 m for the optical bench. Operation with the polarized source could be interleaved with unpolarized source operation. A switching magnet between the RFQ's and the LINAC III would be used to alternate the source of beam on the time scale of the acceleration cycles. This technique is already in use at Brookhaven National Laboratory (BNL) where polarized and unpolarized beam may be accelerated on alternate machine cycles.

Two scenarios for placement of the polarized ion source and RFQ are being considered. The original HERA RFQ used with the magnetron source could be replaced if unpolarized ion source development with the "RF source" is complete and if one operational ion source RFQ assembly is shown to be operationally viable. If the original RFQ were removed and some shielding walls were rearranged, the polarized source, a beam transport line, and a new RFQ could be installed in-line with the LINAC III. The already tested RFQ to LINAC beam line could then be used for polarized beam transport, or a new design could be installed. An area needs to be assigned for the power supplies, the control station, and the optical bench.

An alternate scenario would be to leave the old RFQ and magnetron in place and incorporate a third RFQ. Then the source might be installed in the area of Hall 1. The third RFQ would be coupled to the LINAC III through a three-way dipole magnet to which the other RFQ's are attached. Experience with operation of the new RF source may determine which of the two layouts are chosen.

6.2 20 keV beamline

1. Optics design

Source technology has improved immensely during the last few years. In the SPIN Collaboration's Report to Fermilab [1], expected intensities of polarized H⁻ were about 1.0 mA to 1.5 mA in an emittance of 2.0π mm-mrad. Now, with a neutral beam injector on an OP-PIS, 20 mA may be possible in the same phase space area. With improvements to a resonant charge exchange ionizer atomic beam source (ABPIS), 5 mA could be possible. In order to achieve good matching to the RFQ, the effects of space charge on the beam transport must be considered. The 20 keV transport line should be kept as short as possible and transitions between regions of space charge neutralization and non-space charge neutralization must be minimized. In any case, the short pulse length of the RFQ/LINAC necessitates an electrostatic field throughout the beam transport line in order to achieve consistent beam transport

Figure 6.1. Floor plan for the low energy beam transport

efficiency during the pulse. Excellent vacuum, with pressure in the range of 10^{-7} mbar, is also needed.

The beam would be transported through a bending magnet, after it was extracted from the source. Incorporated into this magnet would be a provision to transport the beam away from the RFQ into a polarimeter. This magnet should be followed by two quadrupole triplets, two sets of x-y steerers integral to the quad triplets, a spin rotator and a set of axially-symmetric Einzel lenses to generate the very small, highly convergent beam for optimum transmission. The first five elements should be installed in such a way as to produce a symmetric beam in x and y at the Einzel lens pair. A similar RFQ, developed for the SSC, has a 35 keV entrance energy, a beam convergence of 140 mrad and a beam size of only 4 mm. The SSC RFQ final energy is 750 keV. Considerable design and development effort to achieve the best beam matching from the source to the RFQ will be necessary.

The spin quantization axis from the polarized source would be either longitudinal (OP-PIS) or horizontal (ABPIS) relative to the beam direction. For an OPPIS, a Wien filter might be required to rotate the spin into the vertical axis. For an ABPIS, a spin rotation solenoid would be required to rotate the spin by 90°. Either device would be installed after the first quadrupole triplet in the 20 keV beam line.

The ion source and LINAC group at BNL will be designing, building and installing a polarized H⁻ ion source and an RFQ for polarized beam injection into RHIC. This development effort should be followed closely and the experience gained at BNL should be used in the design of the HERA polarized beam delivery system.

2. Beam diagnostic systems

A passive toroid and a four quadrant collimator would be installed upstream of the Einzel lens pair. Other diagnostics such as an emittance measuring apparatus, a Faraday cup, and an x-y harp would be installed during commissioning of the beam transport line but removed for normal operation.

3. Vacuum system

A gate valve would separate the source and the RFQ. Pumping will be provided by cryopumps and/or ion pumps to avoid any possible oil contamination of the RFQ. A 500 l/s turbopump cart will be used to pump down the 20 keV and 750 keV beamlines. It will also be used to rough out cryopumps after regeneration.

6.3 750 keV beamline

1. Optics design

a. Transverse beam optics system: In general, beam transport elements between the RFQ and LINAC III must be designed to manipulate the four transverse matching parameters, α_x , β_x , α_y , and β_y . A permanent magnet quadrupole, placed very close to the exit of the RFQ, would improve transmission by decreasing the large x divergence and y convergence before being transported to the first quadrupole triplet. If a bending magnet is added, focusing elements to make the bend doubly achromatic should be included to limit emittance growth.

The two scenarios mentioned above may be considered separately. If the old magnetron RFQ were replaced by the SPIN RFQ, the matching to the LINAC III could be made with existing hardware. Additional pulsed quadrupoles and a dipole may be required in order to switch rapidly between ion sources. Four quadrupoles and two steerers would add enough degrees of freedom to meet the matching criteria but additional elements may be needed to retain the flexibility of switching between sources. Should a third RFQ be added to the transport scheme, it would be connected using a three-way switching magnet. This magnet does not exist and would have to be designed and manufactured. Additional focusing and steering elements would be required to ensure a doubly-achromatic beam transport system. In such a case, it may be necessary to add an additional bend of the same angle to achieve achromatic transport.

b. Longitudinal beam optics system: The RFQ is being designed at IHEP-Protvino to minimize the longitudinal beam emittance; the rms relative energy and phase spreads are $\pm 1.54\%$ and 12.3° . These values are the present limit for commercially available RFQ's, although we hope for an even smaller longitudinal emittance. One buncher is usually required for approximately every meter of beam transport 1 , especially for the higher intensity beams (20 mA) where longitudinal space charge forces become significant.

2. Beam diagnostic systems

- a. Transverse beam diagnostics: Moving slits and a harp located in the beamline after the RFQ would measure the beam emittance. Transverse measurements of the beam during different times within each pulse would be measured using an x-y harp with fast sampling electronics. This would allow an estimate of any emittance growth due to space charge effects upstream of the RFQ.
- **b.** Longitudinal beam diagnostics: A 95% transmission wire grid (longitudinal profile monitor) would be mounted after the RFQ to measure the beam phase spread and as a start signal for a time of flight energy measurement system. A second pick-up would be located close to the LINAC.

¹Private communication, Deepak Raparia, BNL

3. Vacuum

Gate valves would separate the RFQ and the main 750 keV beam line vacuum systems. Pumping will be provided by one or two cryopumps.

6.4 Beam switching and control system

To switch between polarized and unpolarized beam, one dipole, several quadrupoles and several steerers must be switched to different operating currents. The cost of this switching system is not included in the cost estimate.

The control system requirements for the beamline and polarized ion source would be specified by the SPIN Collaboration, but would be built at DESY to ensure complete compatibility with the present control system. There should be a control console in the ion source area to facilitate the ion source and beamline commissioning.

6.5 RFQ

Table 6.1. RFQ-0.75 specifications

Table 6.1. RFQ-0.75 specifications.				
operating frequency	$201.25~\mathrm{MHz}$			
ion type	polarized ${ m H}^-$			
input energy	$20 \mathrm{keV}$			
output energy	$750~{ m keV}$			
cavity length	$162~\mathrm{cm}$			
cavity diameter	$36~\mathrm{cm}$			
number of cells in vane $(\beta \lambda/2)$	156			
vane thickness	$6~\mathrm{mm}$			
vane length (including matching part)	$152.0~\mathrm{cm}$			
intervane voltage	$60~\mathrm{kV}$			
peak surface field	$22 \mathrm{\ MV/m}$			
average radius (R_0)	$3.90~\mathrm{mm}$			
minimum bore radius	$2.80~\mathrm{mm}$			
the maximum modulation (R_{max}/R_{min})	1.79			
acceleration efficiency	0.001 to 0.390			
input synchronous phase	-90°			
output synchronous phase	-30°			
operating current	1-15 mA			
current limit	27 mA			
transmission	99%			
energy spread (95% of the beam)	2.4%			
phase width (95% of the beam)	18°			
acceptance (at 1.6 mA)	$2.4~\pi$ mm mrad			
dissipative power	60 kW			

A high transmission efficiency Radio Frequency Quadrupole (RFQ-0.75) was designed in IHEP-Protvino [1] for accelerating polarized H⁻ beam to 750 keV for Fermilab. It would consist of an accelerating structure and an rf power supply.

To achieve the required transmission efficiency of nearly 100%, IHEP-Protvino investigated various RFQ structures and optimized them for reducing the energy spread without reducing the transmission efficiency. These efforts were somewhat successful. Some characteristics of the optimized RFQ are listed in Table 6.1.

The basic AGS RFQ parameters [2] were used at the beginning of the design study. The RFQ accelerating structure was then optimized to achieve maximum performance. It was found that the 2H accelerating cavity structure has several advantages over 4V cavities [3]; thus the 2H cavity was chosen for the RFQ-0.75 design.

The RFQ design can take advantage of the lower polarized ion source current (<20 mA). It was optimized to reduce the output energy spread; this could reduce beam losses in the 750 keV beam transfer line and could allow better matching with the existing DESY LINAC. The output energy spread of $\pm 1.2\%$ was achieved by decreasing, at the RFQ's low energy end, the acceleration efficiency $\theta(n)$, where n is the cell number [4]. Strong Coulomb forces in the bunch core of an accelerated beam could increase the output energy spread. To minimize this effect, the space charge density was reduced by turning off $\theta(n)$ and thus the focusing in several accelerating cells. A numerical tracking was used to find an optimum solution. The best results for the 156 cell RFQ were obtained with $\theta(n)$ set to zero in cells 15 to 25 and cells 66 to 68.

It was recently suggested that increasing the source energy from 20 keV to about 50 keV could significantly increase the geometrical acceptance of the RFQ. After further study, this change may be recommended.

6.6 Cost Estimate

Table 6.2. An estimate of the costs for the new low energy beam line.

System	Estimated Cost
Vacuum	DM 120 k
20 keV beamline lenses and power supplies	DM 100 k
750 keV beamline lenses and power supplies	DM 120 k
Control system	DM 75 k
Bunchers (1 or 2)	DM 130 k
Beam diagnostic systems	DM 90 k
Beam line assembly	DM 15 k
RFQ and power supply	DM 600 k
Hardware Total	DM 1200 k
Building Construction	$\mathrm{DM}\ 300\ \mathrm{k}$

References

- [1] SPIN Collaboration, "Acceleration of polarized protons to 120 GeV and 1 TeV at Fermilab", University of Michigan Report UM-HE 95-09 (1995).
- [2] F.Z. Khiari et al., Phys. Rev. **D39**, 45 (1989).
- [3] O.K. Belyaev and V.B. Stepanov, IHEP Preprint 91-126, Protvino (1991).
- [4] Y.Budanov, A.Zherebtsov, "On Dynamics of the Longitudinal Emittance in RFQ", Proc. 1st BDO Workshop, St.Peterburg (1994).

7 DESY III polarized beam hardware (7.5 GeV/c)

Polarized protons encounter many depolarizing resonances during acceleration in high energy proton synchrotrons. Normally an unperturbed proton's spin precesses around the ring's vertical magnetic field. The spin tune ν_s , which is the number of spin rotations that occur during one revolution around the ring, is normally proportional to the Lorentz factor γ :

$$\nu_s = G\gamma \tag{7.1}$$

where G=1.792847 is the proton's anomalous magnetic moment. This vertical spin precession becomes unstable when the spin precession frequency is synchronized with some harmonic frequency of even a small horizontal perturbation field. Such resonant perturbations can depolarize the beam in a circular accelerator and are called spin depolarizing resonances. During acceleration a large number of depolarizing resonances are crossed, whenever $G\gamma$ passes through a depolarizing resonance spin tune.

Two types of horizontal perturbation fields can cause depolarizing resonances. The imperfection fields of the accelerator lattice can cause imperfection depolarizing resonances. These occur when the spin tune becomes equal to an integer n; then the n-th harmonic perturbing field has a coherent depolarizing effect during each turn around the ring. These $G\gamma = n$ imperfection depolarizing resonances occur every 523 MeV during the acceleration cycle.

Intrinsic depolarizing resonances exist even in an ideal accelerator lattice because the protons oscillate vertically around the closed orbit, thus passing off-axis through the quadrupoles' horizontal fields. These intrinsic resonances occur when the vertical betatron oscillation frequency, $f_c\nu_y$, is synchronized with the protons' spin precession frequency, $f_cG\gamma$, where f_c is the circulation frequency. Thus, these intrinsic resonances are crossed when γ satisfies

$$G\gamma = n \pm k\nu_y , \qquad (7.2)$$

where k and n are integers. The strongest first order intrinsic resonances in DESY III occur for k=1 and n=mP, where P=8 is the number of superperiods in the DESY III. In the DESY III cycle, which accelerates protons from T=50 MeV to 7.5 GeV/c, there is probably only one strong imperfection resonance, at $G\gamma=8$, and four strong intrinsic resonances as shown in Table 7.1.

We calculated the strength of the depolarizing resonances in the DESY III synchrotron using the program DEPOL [1]. It sums the effect of all the lattice elements into a single depolarizing force. The intrinsic depolarizing resonances strengths were computed for a proton beam with a vertical betatron tune of 4.303 and a normalized 2σ beam emittance of 20π mm-mrad containing 86% of the beam; this estimates the resonance strength for the maximum betatron oscillation amplitude for this emittance. The strength of each imperfection resonance is proportional to the rms closed orbit error; we calculated the imperfection resonances' strengths assuming a random magnet misalignment that causes a 3 mm rms closed orbit error in the vertical plane. The resulting resonance strengths ϵ for DESY III's five strong resonances are given in Table 7.1.

$=G\gamma$	γ	$T (\mathrm{GeV})$	P (GeV/c)	ϵ
	4.462	3.247	4.08	0.0130
$-\nu_u$	2.062	0.996	1.69	0.0026

2.05

6.05

6.37

0.0102

0.0070

0.0090

Table 7.1. Strongest depolarizing resonances in DESY III.

1.313

5.184

5.500

Note that the present DESY III unpolarized proton beam emittance is about 20π mmmrad and present closed orbit rms error is about 3 mm. Hopefully the polarized ion source emittance may be smaller than the unpolarized emittance. Moreover, these parameters might be improved for both polarized and unpolarized protons by modest improvements in the hardware and accumulation techniques in DESY III, PETRA, and HERA.

7.1 Overcoming depolarizing resonances in DESY III

2.400

6.525

6.862

 $16 - \nu_y$

The depolarization caused by spin resonances can be avoided by installing an optically transparent Siberian snake in an accelerator. By rotating the spin of each proton 180° around a horizontal axis, a full Siberian snake could effectively overcome all first order depolarizing resonances. However, in a medium energy machine such as the DESY III synchrotron a full snake could strongly perturb the beam dynamics. Fortunately the number of resonances in DESY III is small and individual resonance correction methods could be used in combination with a partial Siberian snake. A partial Siberian snake, which rotates the spin by a fraction of 180°, allows one to compensate for the effect of all imperfection resonances. The partial snake concept was successfully tested at IUCF [3] and at the AGS [4]. The strength of the partial snake solenoid in DESY III must be significantly larger than twice the maximum imperfection resonance strength [2]; thus its spin precession angle ϕ must obey

$$\phi \gg 2\pi |\epsilon_{imp}| + \sqrt{8\pi\alpha} , \qquad (7.3)$$

where ϵ_{imp} is the maximum imperfection resonance strength and α is the resonance crossing speed given by

$$\alpha = \frac{1}{2\pi f_c} \left(\frac{d\gamma}{dt} \pm k \frac{d\nu_y}{dt} \right). \tag{7.4}$$

Note that the second term appears only for intrinsic depolarizing resonances. The strongest imperfection resonance in DESY III is $G\gamma = 8$ with $\epsilon = 0.0130$; therefore a 5% partial Siberian snake should be sufficient to overcome all imperfection depolarizing resonances in the DESY III. A warm rampable solenoid similar to the one proposed for the Fermilab Booster [7] could be built for the DESY III partial snake.

The intrinsic depolarizing resonances in DESY III can not be overcome by a 5% partial Siberian snake. Instead, one could use the fast betatron tune jump technique, as at the ZGS [7] and the AGS [8], or one could decrease the resonance crossing rate, as at Saturne [9].

Both methods would change the resonance crossing speed to preserve the polarization. For a constant crossing speed α , the final polarization P_f is related to the initial polarization P_i by [5]

 $P_f = P_i \left[2 \exp\left(\frac{-\pi \epsilon^2}{2\alpha}\right) - 1 \right], \tag{7.5}$

where ϵ is the depolarizing resonance strength. Equation 7.5 indicates that the polarization should be preserved if $\epsilon^2/\alpha \to 0$ (weak resonance or fast resonance crossing) or if $\epsilon^2/\alpha \to \infty$ (strong resonance or slow resonance crossing).

A recent experiment at IUCF [11] indicates that one can spin flip through an intrinsic resonance not only by making the resonance crossing rate slow but also by increasing the resonance strength with a vertical beam kicker magnet. A short dipole pulse could excite a coherent vertical beam oscillation, which would make the intrinsic resonance several times stronger. The experimental data are shown on Fig. 7.1, where the polarization after crossing the resonance is plotted against the strength of the beam kick; clearly the spin flips for large $\int B \cdot d\ell$. This method could be significantly cheaper than the pulsed-quadrupole method, which requires expensive power supplies and long tuning for a precise timing of a tune jump. Note that the coherent betatron oscillations excited by a vertical kicker could increase the beam emittance. Thus, a feedback or cooling system may be needed to damp the beam after each kick to avoid emittance blow-up. Further study is necessary to choose which method would be the best for overcoming the intrinsic depolarizing resonances in DESY III.

Figure 7.1. Polarization after crossing the $G\gamma = 7 - \nu_y$ intrinsic depolarizing resonance is plotted against the strength of the kicker magnet [11].

In summary, in the DESY III synchrotron, which probably has only a few strong depolarizing resonances, beam polarization could be maintained by using:

- one partial snake to overcome imperfection resonances,
- several pulsed quadrupoles to jump the four intrinsic resonances or a kicker magnet with a feedback to spin flip through the intrinsic resonances.

Figure 7.2. DESY III with polarized beam hardware.

7.2 Cost Estimate

Possible locations for the polarized beam hardware in DESY III are shown in Fig. 7.2. We estimate that the partial snake solenoid would cost about **DM 200** k, while the pulsed quadrupoles with power supplies would cost about **DM 300** k; a kicker magnet system would cost about **DM 100** k plus the cost of a possible feedback or cooling system.

References

- [1] E.D. Courant and R. Ruth, BNL Report BNL-51270 (1980).
- [2] T. Roser, AIP Conf. Proc. 187, 1442 (1988).
- [3] V.A. Anferov et al., Phys. Rev. 46, R7383 (1992);
 B.B. Blinov et al., Phys. Rev. Lett. 73, 1621 (1994).
- [4] H. Huang et al., Phys. Rev. Lett. 73, 2982 (1994).
- [5] M. Froissart and R. Stora, Nucl. Inst. Meth. 7, 297 (1960).
- [6] D. Cohen, Rev. Sci. Instrum. 33, 161 (1962).
- [7] T. Khoe et al., Particle Accelerators 6, 213 (1975).
- [8] F. Z. Khiari et al., Phys. Rev. **D39**, 45 (1989).
- [9] J.L. Laclare et al., J. Phys. (Paris), Colloq. 46, C2-499 (1985);
 P.A. Chamouard et al., Colloq. Phys. 51, C6-569 (1990).
- [10] SPIN Collaboration, "Acceleration of polarized protons to 120 GeV and 1 TeV at Fermilab", University of Michigan Report UM-HE 95-09 (1995).
- [11] D.A. Crandell et al., Phys. Rev. Lett. 47, 1763 (1996).

8 PETRA polarized beam hardware (40 GeV/c)

To accelerate a polarized proton beam to 40 GeV/c in PETRA one must overcome many spin depolarizing resonances. Fortunately, the Siberian snake technique [1] should cancel the effect of all depolarizing resonances by rotating the proton spin by 180° around a horizontal axis. The Siberian snake experiments [2] at the IUCF Cooler ring suggest that this method could overcome all depolarizing effects at 40 GeV/c.

8.1 Depolarizing resonance strength

The strengths $\epsilon_{\rm int}$ and $\epsilon_{\rm imp}$ of the intrinsic and imperfection depolarizing resonances in the PETRA ring were calculated with the DEPOL program [3] for a vertical betatron tune of 11.23 and assuming a 2σ polarized beam normalized emittance of 25 π mm-mrad and an RMS closed orbit distortion of 2.2 mm. The resulting intrinsic depolarizing resonance strengths are shown in Fig. 8.1. The maximum imperfection resonance strength is similar to the intrinsic resonance strength: $\epsilon_{\rm int} = 0.06$ and $\epsilon_{\rm imp} = 0.04$. The required number of snakes N is proportional to the maximum strength of the intrinsic resonances [4]:

$$N > \epsilon_{\text{int}} \cdot 5$$
 . (8.1)

Therefore, one Siberian snake should be sufficient to overcome all PETRA depolarizing resonances. However, with one Siberian snake in the ring the stable polarization direction lies in the horizontal plane. This would make it difficult to monitor the beam polarization

Figure 8.1. The intrinsic resonance strengths vs. γ for the PETRA ring assuming 25π mm·mrad normalized emittance.

during acceleration and would complicate spin manipulation during injection and extraction. We therefore suggest using two snakes in PETRA, which would give a significant safety factor in spin stability and would also simplify the polarization monitoring and beam extraction. Two snakes in PETRA would make the stable polarization direction vertical and would make the spin tune entirely energy-independent.

8.2 Siberian snake configuration in PETRA

Even though a single snake is the most simple option, it has several disadvantages. There would be no special requirement on the snake's location in PETRA or on its spin rotation axis; this axis could be used as a free parameter for the snake design optimization. However, the stable spin direction would be horizontal and energy dependent except opposite to the snake location, where it is always directed along the snake axis. The polarization could be made vertical, for the beam polarization measurements, by turning the snake off adiabatically at energies corresponding to a half integer value of $G\gamma$ [5].

The two snakes option seems more appropriate for PETRA. One could place the two Siberian snakes exactly opposite to each other in the PETRA ring; thus they would be separated by 180° or exactly 1/2 of the total $\int B \cdot d\ell$ of the ring magnets. This would make the spin tune energy-independent during acceleration from 7.5 to 40 GeV/c.

The overall layout of the polarization hardware in PETRA was shown in Figure 1.1. Figure 8.2 shows possible snake locations in the North and South straight sections of PETRA.

Figure 8.2. South and North straight sections in PETRA with possible snake locations.

The value of the spin tune would be determined by the angle between the two snakes' spin rotation axes. It would be best to have the two snakes' spin rotation axes perpendicular to each other; this would force PETRA's spin tune ν_s to be exactly 1/2. If the snakes' spin precession axis is 45° from the beam axis, then one could use two physically identical snakes with identical magnets; only the currents would be opposite.

There is also another option for PETRA. One could start with one snake at injection (or inject the beam and turn the first snake on); while the second snake could be ramped up during the acceleration. The two snakes would have different designs: one would be longitudinal and one would be radial. These snakes would have smaller apertures, but would require two different designs and the accelerator operation would be more complex.

At present we consider two warm fully-on Siberian snakes with $\pm 45^{\circ}$ axes to be a good choice for PETRA; this would simplify the operation and minimize the modifications to the existing accelerator. A single snake design could serve for both snakes by reversing the current.

8.3 Siberian snake design

A full Siberian snake must rotate the spin by 180° around a horizontal axis without perturbing the beam orbit outside of the snake. At very high energies, transverse magnetic fields are much more effective in rotating the spin, because of the invariance of their $\int B \cdot d\ell$ under the Lorentz transformation. The transverse magnetic fields cause orbit excursions inside the snake magnets; fortunately these excursions decrease with increasing energy. For medium-energy accelerators, such as PETRA, designing a transverse snake is somewhat difficult because the orbit excursions are fairly large at 7.5 GeV/c injection. Moreover, the snake design is constrained by the space available in the PETRA straight sections.

A practical Siberian snake can be constructed using some sequence of dipole magnets; it rotates the spin by 180 degrees around a horizontal axis while restoring the beam to its normal orbit outside the snake (optical transparency). The disadvantage of such a discrete snake is a fairly large orbit excursion at low energies. The warm seven-dipole Steffen-Lee snake [6] with a 45° axis would require more than a 40 cm vertical aperture at 7.5 GeV/c [7].

An alternative is to use a long dipole magnet twisted into a helix. Snakes using helical dipoles have the advantage of smaller orbit excursions at low energies, such as PETRA's 7.5 GeV/c injection energy. A 10% model helical dipole magnet was built at IHEP-Protvino demonstrating the possibility of constructing a full scale helical magnet [7]. A single twist helical snake with two orbit correction dipoles on each side shown in Fig. 8.3 was considered for the Fermilab Main Injector; it had a 34° spin rotation axis and orbit excursion of about 16 cm at 8.9 GeV/c. This helical design could be used for the PETRA snakes. The total length of the snake is 14.5 m while the distance between quadrupoles in the PETRA straight sections is typically 7 m. Therefore, the optics of two opposite straight sections must be slightly changed to accommodate a warm snake.

Another possible helical snake configuration for PETRA is shown in Fig. 8.4. It consists



of a vertically bending magnet surrounded by two helical dipoles and two correction dipoles. The largest orbit excursion would then be in the central dipole; this would still allow a fairly inexpensive magnet since the large excursion would be perpendicular to the magnet's field direction. This snake would have a 45° spin rotation axis and would be about 13 m long with a 2 T maximum field. Both snake configurations described above certainly need further study to optimize the warm snake design for PETRA.

RHIC [8] is now developing superconducting helical snakes; a similar superconducting helical snake could certainly be designed for PETRA. Another alternative would be a superconducting dipole snake somewhat similar to the design shown in Fig. 10.5 of this report. Either superconducting snake in PETRA would significantly reduce both the orbit excursions and the power consumption. However, it would be expensive to install helium transfer lines from the two opposite snake positions in the warm PETRA ring to the main helium transfer line in HERA. One might instead consider installing a helium storage dewar near each superconducting PETRA snake, which would be filled perhaps once per week.

The choice between these alternatives should be based on minimizing the total cost of construction plus operation for perhaps 5 years. In Figs. 8.3 and 8.4 we have considered only warm snake because of our limited time to finish this report; however we are not sure that this is the best choice.

8.4 Conclusion

We conclude that two full Siberian snakes in PETRA should overcome all depolarizing resonances and maintain vertical polarization during the acceleration to 40 GeV/c. The two snakes would be located on opposite sides of the ring in the North and South straight sections and would not cause any significant optics change to the present lattice. Both snakes would have identical design with 45° spin rotation axis but opposite currents to set the spin tune at 1/2 away from all depolarizing perturbations. The snakes would probably use helical dipole magnets to minimize the orbit excursions inside each snake at injection. Also note that further optimization of the snake design could be made and alternative snake configurations should be considered. Future studies should also include numerical spin tracking and stroboscopic averaging to maximize the spin stability during the whole acceleration cycle.

8.5 Cost Estimate

We estimate that the warm helical magnet snakes would each cost about **DM 500** k plus about **DM 150** k for the warm snake's power supply. We estimate that these snakes would require about 12 months to produce once the design is finalized.

References

- [1] Ya. S. Derbenev and A. M. Kondratenko, Sov. Phys. Doklady 20, 562 (1976).
- [2] A.D. Krisch et al., Phys. Rev. Lett. 63, 1137 (1989);
 J. Goodwin et al., Phys. Rev. Lett. 64, 2779 (1990).
- [3] E. D. Courant and R. Ruth, BNL Report BNL-51270 (1980).
- [4] S. Y. Lee and E. D. Courant, Phys. Rev. **D41**, 292 (1990).
- [5] R.A. Phelps et al., Phys. Rev. Lett. 72, 1479 (1994).
- [6] K. Steffen, Part. Accel. 24, 45 (1989); S. Y. Lee, Nucl. Instrm. and Meth. A306, 1 (1991).
- [7] SPIN Collaboration, "Acceleration of polarized protons to 120 GeV and 1 TeV at Fermilab", University of Michigan Report UM-HE 95-09 (1995).
- [8] Y. I. Makdisi, in Proc. of the 11th International Symposium on High Energy Spin Physics, 1994 Bloomington, 1, 75 (1995).

9 The polarization in HERA

In order to maximize the number of collisions of stored particles in a storage ring system one tries to maximize the total number of particles in the bunches and tries to minimize the emittances so that the particle distribution across phase space is narrow and the phase space density is high. Furthermore, the beam should ideally be at equilibrium i.e. the phase space distribution should be periodic in the machine azimuth.

If, in addition, the beam is spin polarized, one requires that the polarization is high and in equilibrium. The polarization state of a spin 1/2 stored beam at equilibrium is defined by the phase space density distribution, the value of the equilibrium polarization at each point in phase space, and the direction of the equilibrium polarization at each point. Once we know these three functions we have a complete specification of the polarization state of the beam.

The maximizing of the polarization of the ensemble implies two conditions:

- 1. The polarization at each point in phase space should be high.
- 2. The equilibrium polarization vector at each point in phase space should be almost parallel to the average polarization vector of the beam.

Indeed, as we will show later, in the HERA proton ring it can happen that on average the equilibrium polarization vector deviates by tens of degrees from the average polarization vector of the beam. Thus even if each point in phase space were 100% polarized the average polarization could be limited to a value much smaller than 100%. The first condition requires that the source delivers high polarization and that the polarization is maintained during acceleration. The second condition is an intrinsic property of the arrangement of the magnets in the ring, the energy, and the optic. At the interaction points the average direction should, of course, be oriented according to the requirements of the experiments. If it were to be demonstrated that the ring and the optic do not permit a high parallelism, there would be little point in striving to fulfill condition 1.

This chapter is an extract from [1]. It deals with a perfectly aligned machine and can only serve to give a first impression. Much of the background has been covered in several other reports [2, 3, 4, 5, 6] and they should be consulted for mathematical details. Furthermore, an extensive study based mainly on long term spin-orbit tracking can be found in [7]. This also gives examples of spin-orbit motion for various Siberian Snake schemes. This study, including a resonance strength analysis, indicated how problematic accelerating and storing polarized protons in HERA can be. We therefore derived a more direct method of looking at spin stability [5] which leads to the results of this section.

9.1 The equilibrium polarization direction

Spin precession for particles traveling in electric and magnetic fields is described by the Thomas-Bargmann-Michel-Telegdi (T-BMT) equation [8, 9]:

$$\frac{d\vec{S}}{ds} = \vec{\Omega} \times \vec{S} \tag{9.1}$$

where $\vec{\Omega}$ depends on the electric and magnetic fields, the velocity and the energy. In magnetic fields at high energy equation (9.1) can be written as

$$\frac{d\vec{S}}{ds} = \frac{e\vec{S}}{mc\gamma} \times \{(1+G)\vec{B}_{\parallel} + (1+G\gamma)\vec{B}_{\perp}\} , \quad G = \left(\frac{g-2}{2}\right)$$
 (9.2)

where \vec{B}_{\parallel} and \vec{B}_{\perp} are the magnetic fields parallel and perpendicular to the trajectory, s is the arc length and the other symbols have the usual meanings. The gyromagnetic anomaly $G = \frac{g-2}{2}$ for protons is about 1.79. The full T-BMT equation contains terms depending on the electric field but these vanish if the electric field is parallel to the velocity. This is the case in radio frequency cavities in a first approximation. The T-BMT equation shows that in one turn around the design orbit of a flat storage ring a non-vertical spin precesses $G\gamma$ times. We call this latter quantity the 'naive spin tune' and denote it by ν_0 . It gives the natural spin precession frequency in the vertical dipole fields of the ring. At 820 GeV, ν_0 is about 1557. The 'naive spin tune' is to be distinguished from the 'real spin tune' which must be used for calculations in rings with exotic magnet elements.

In horizontally bending dipoles, spins precess only around the vertical field direction. The quadrupoles have vertical and horizontal fields and therefore additionally cause the spins to precess away from the vertical direction. The strength of the spin precession and the precession axis in machine magnets depends on the trajectory and the energy of the particle. Thus in one turn around the ring the effective precession axis can deviate from the vertical and will depend on the initial position of the particle in six dimensional phase space. From this it is clear that if an equilibrium spin distribution exists, i.e. if the polarization vector at every phase space point is periodic in the machine azimuth, it will vary across the orbital phase space.

We denote the polarization at each point \vec{z} in six dimensional phase space and at azimuth θ by $\vec{\mathcal{P}}(\vec{z},\theta)$. Since the T-BMT equation is linear in the spin, $\vec{\mathcal{P}}(\vec{z},\theta)$ obeys the T-BMT equation [10] which we now write in the form

$$\frac{d\vec{\mathcal{P}}}{d\theta} = \vec{\Omega}(\vec{z}, \theta) \times \vec{\mathcal{P}} . \tag{9.3}$$

Because equation (9.3) describes precession, $|\vec{\mathcal{P}}(\vec{z},\theta)|$ is constant along a phase space trajectory.

At equilibrium, $\vec{\mathcal{P}}(\vec{z}, \theta)$ not only obeys the T-BMT equation, but it is also periodic in θ . We write the equilibrium $\vec{\mathcal{P}}$ as $\vec{\mathcal{P}}_{eq}$ and we denote the unit vector along $\vec{\mathcal{P}}_{eq}(\vec{z}, \theta)$ by $\vec{n}(\vec{z}, \theta)$. Obviously \vec{n} also obeys equation (9.3) and thus behaves like a spin. The vector \vec{n} was first introduced by Derbenev and Kondratenko [11] in the theory of radiative electron polarization. By its definition the field of equilibrium spin directions in phase space does not change from turn to turn when particles propagate through the accelerator. However, after each turn individual particles find themselves at new positions in phase space. Thus the periodicity condition implies that when a particle at an initial phase space point \vec{z}_i is transported to a final point \vec{z}_f during one turn around the storage ring we have

$$\underline{R}(\vec{z}_i, \theta) \vec{n}(\vec{z}_i, \theta) = \vec{n}(\vec{z}_f, \theta) . \tag{9.4}$$

where $\underline{R}(\vec{z}_i, \theta)$ is the orthogonal spin transport matrix for one turn on that orbit.

Clearly, it is very important to have accurate and efficient methods for calculating $\vec{n}(\vec{z}, \theta)$. Note that $\vec{n}(\vec{z}, \theta)$ is usually not an eigenvector of the spin transfer matrix at some phase space point since the spin of a particle changes after one turn around the ring, but the eigenvector would not change.

We expect that the spins would reach their equilibrium distribution simply as a result of the adiabatic acceleration process [2].

9.2 The HERA lattice

In this section we describe the model for the HERA ring used in our calculations.

The HERA ring has a circumference of about 6.335 kilometers. There are a total of one hundred FODO cells in the arcs and the phase advance per cell is 90 degrees in both planes. In anticipation of field nonlinearities due to persistent currents in the superconducting magnets, multipole correction windings are built into many of the magnets. For the calculations presented here nonlinear fields and skew fields are ignored. The orbit motion is linearized.

A further aspect of the HERA proton ring and one that has totally nontrivial implications for spin motion is that there are sets of interleaved vertical and horizontal bends on each side of the North, South, and East interaction points. These serve to adjust the height of the proton ring to that of the electron ring at the collision points. Coming from the arc, a proton is first bent 5.74 milliradians downwards, then 60.4 milliradians towards the ring center and finally the orbit is made horizontal by a 5.74 milliradians upward bend. The structure is repeated with interchanged vertical bends on the far side of the interaction point at the entrance to the arc.

It is easy to see that with $G\gamma \approx 1557$ the interleaved vertical and horizontal bends cause a massive disturbance to the spin motion. In a perfectly aligned ring without vertical bends the equilibrium spin direction on the design orbit, $\vec{n}_0 = \vec{n}(0, \theta)$ is vertical. With vertical bends \vec{n}_0 is no longer vertical and strongly energy dependent.

In the West area there is no interaction point for collisions with electrons and positrons. So there are no vertical bends. Our calculations are based on the 1996 luminosity optic. This optic and the magnets are not symmetric with respect to the center of the West area owing to the presence of the HERA-B experiment and beam dump magnets. However, in these calculations the vertical bump associated with the beam dump mechanism is switched off so that the design orbit is horizontal across the whole West area.

The betatron tunes are $Q_x \approx 31.279$ and $Q_z \approx 32.273$. The synchrotron tune at full energy is about 0.000625. For these calculations the invariant one sigma emittance ϵ_{σ} is taken to be $4\pi \cdot 10^{-6}$ meter radians in both planes; this value is obtained under optimum conditions. The invariant one sigma emittance is defined to be $\gamma v/c$ times the area of an upright ellipse passing through the phase space point $(x = \sigma, x' = 0)$. This area $\epsilon_{\sigma}/(\gamma v/c)$ is equal to $\pi \sigma^2/\beta$; β is the optical beta function, γ is the relativistic factor, and v/c is the velocity. For Gaussian beams the one sigma ellipse contains 39% of the beam in each dimension. The fractional ('1 sigma') energy spread is about $5 \cdot 10^{-5}$. However, synchrotron oscillations are not considered in this report.

Figure 9.1. Propagation of a beam that is initially completely polarized parallel to \vec{n}_0 leads to a fluctuating average polarization. For another beam that is initially polarized parallel to the periodic spin solution \vec{n} the average polarization stays constant, in this case equal to 0.765.

9.3 Computational techniques

9.3.1 Straightforward polarization tracking

One can try to get information about the spread of the equilibrium spin directions over phase space by tracking a completely polarized beam for many turns. This is illustrated in figure 9.1. There are no geometrical distortions and the vertical bends are turned off so that the simulation represents a perfectly aligned flat ring. Particles at 100 different phases on a 1 sigma vertical phase space ellipse and zero longitudinal and horizontal emittance have been tracked through HERA for 600 turns while the beam was initially 100% polarized parallel to \vec{n}_0 . Similar kinds of tracking results have been presented in [7]. The polarization of the ensemble is defined as the average across the phase space of the unit spin vectors. We see that the polarization oscillates wildly. This polarization distribution is obviously not an equilibrium distribution and this implies that the \vec{n} -axes are widely spread out away from \vec{n}_0 . The bold horizontal line is the turn by turn polarization obtained when each spin is initially set parallel to $\vec{n}(\vec{z},\theta)$ (calculated using the code SPRINT-see below) at its phase space position \vec{z} . Now the averaged polarization stays constant at 0.765. This latter value is consistent with the fact that the average opening angle is about 40 degrees. Therefore, by starting simulations with spins parallel to the \vec{n} -axis one can perform a much cleaner analysis of beam polarization in accelerators. In effect one is now able to study the effect of spin perturbations (for example due to field noise, beam-beam effect etc) by searching for small deviations away from the 'stationary state' of the beam instead of having to detect long term drifts in a strongly fluctuating average polarization.

9.3.2 The linear (SLIM) theory

A well established and often justified procedure is to linearize the orbit motion. A spin can be parameterized by two angles describing its tilt away from \vec{n}_0 . Under some circumstances one can additionally linearize with respect to these angles. This is the basis of the code SLIM for calculating electron spin diffusion [12]. \vec{n} can similarly be calculated in linear approximation [13]. However, since \vec{n} in a very high energy accelerator such as HERA can be widely spread out away from \vec{n}_0 , the two angles can be large. In this case this linearization is not justified. Nevertheless the technique has been used to get a first indication that the equilibrium polarization in the HERA proton ring could be limited due to a large spread of the opening angle [2].

9.3.3 Nonlinear normal form analysis

Nonlinear normal form theory provides solutions of equation (9.4) beyond first order by computing the Taylor expansion of $\vec{n}(\vec{z}, \theta)$ with respect to \vec{z} . Theoretically the evaluation order is not limited, but computational errors typically limit the normal form approach to fifth order. Experience has shown that except when the spread of polarization directions is small, this method diverges and a nonperturbative method is needed. When the spread has already been reduced by some means, normal form analysis has been successfully applied in the filtering method mentioned below [4].

9.3.4 Stroboscopic averaging

However, in order to handle the general case we have developed a new method for obtaining \vec{n} called stroboscopic averaging [5]. It is based on multi-turn tracking and the averaging of a special choice of the spin viewed stroboscopically from turn to turn. Since this innovative approach only requires tracking data from one particle, it is fast and very easy to implement in existing tracking codes. Probably the main advantage over other methods is the fact that stroboscopic averaging does not have an inherent problem with either orbit or spin orbit resonances due to its nonperturbative nature. This allows the analysis of the periodic spin solution close to resonances. This algorithm has been implemented in the program SPRINT [5]. This is the code used to calculate the initial \vec{n} -axes needed to propagate the equilibrium distribution in figure 9.1.

The stroboscopic average has a very simple physical interpretation which illustrates its practical importance. If a particle beam is approximated by a phase space density, disregarding its discrete structure, then we can associate an arbitrary spin field $\vec{\mathcal{P}}(\vec{z},\theta_0)$ with the particle beam at the azimuth θ_0 . If one installs a point like 'gedanken' polarimeter at a phase space point $\vec{z}_0 = \vec{z}(\theta_0)$ and azimuth θ_0 , then this polarimeter initially measures $\vec{\mathcal{P}}(\vec{z}_0,\theta_0)$. When the particle beam passes the azimuth θ_0 after one turn around the ring, the polarimeter measures

$$\underline{R}(\vec{z}(\theta_0 - 2\pi), \theta_0 - 2\pi) \cdot \vec{\mathcal{P}}(\vec{z}(\theta_0 - 2\pi), \theta_0) . \tag{9.5}$$

After the beam has traveled around the storage ring a large number of times and the polarization has been measured whenever the beam passed the 'gedanken' polarimeter, one

Figure 9.2. A schematic layout of the interleaved horizontal and vertical bending magnets near the North, South and East interaction points of HERA. The arrows indicate the orientation of the precession axes. If one places a radial Siberian Snake (indicated by the thick arrow) at the midpoint of the four equal horizontal bends one obtains a radial Siberian Snake.

averages over the different measurements to obtain $\langle \vec{\mathcal{P}} \rangle$. In [5] it has been proved that this average is parallel to $\vec{n}(\vec{z}_0, \theta_0)$. If the particles of a beam are polarized parallel to $\vec{n}(\vec{z}, \theta_0)$ at every phase space point, then the spin field of the beam is invariant from turn to turn due to the periodicity property in equation (9.4). But in addition, even for beams which are not polarized parallel to \vec{n} , we see that the polarization observed at a phase space point \vec{z} and azimuth θ_0 is still parallel to $\vec{n}(\vec{z}, \theta_0)$, if one averages over many measurements taken when the beam has passed the azimuth θ_0 .

9.4 Limits to the polarization in HERA

This section describes calculations of the \vec{n} -axis for a perfectly aligned HERA.

As we pointed out above, the spin motion in HERA is complicated by the presence of interleaved vertical and horizontal bends. If we require that \vec{n}_0 is vertical in the arcs at all energies, the vertical bends must be compensated. One way to do this, proposed by V. Anferov [15], would be to insert a radial Siberian Snake at the midpoint of the 60.4 mrad horizontal bends (see figure 9.2). Owing to their special purpose, we will refer to these devices as flattening snakes (FS). The complete magnet system spanning the vertical bends on one side of an interaction point then rotates spins by 180 degrees around the radial direction independently of the energy and therefore also behaves like a Siberian Snake. The spin rotation from the system on the upstream side of the interaction point compensates that from the downstream side so that the non-flat straight sections are transparent to spins on the closed orbit and \vec{n}_0 is vertical in the arcs. For the calculations presented here the vertical bends are switched off in the East corresponding to a geometry in which the proton beam remains at fixed height in the East area. Thus no FS's are needed there. In the full report [1] the case of the non-flat East area is also considered. All snake-like elements are modeled by thin lenses which have no effect on the orbit and rotate all spins by 180 degrees independently of their positions in phase space. Clearly, at a later stage, realistic descriptions of snake fields will be needed.

Figure 9.3. Average opening angle of the equilibrium polarization distribution for particle energies between 814 and 822 GeV with four flattening Siberian Snakes to make the North and the South straight sections spin transparent for particles on the closed orbit. The two curves refer to particles with one sigma in the horizontal direction and one or three sigma in the vertical direction respectively.

9.4.1 HERA without Siberian Snakes

Figure 9.3 (solid curve) shows the average angular deviation of \vec{n} from its average (over the phase space) at the midpoint of the East interaction region for the layout just described and for particles distributed uniformly around the 1 sigma vertical and horizontal phase space ellipses. The calculation was made at fixed energies in the range 814–822 GeV and the angle is measured in radians. Synchrotron motion is not included. We see very strong variations of the opening angle with the minimum lying at about 60 mrad and the maximum at about 90 degrees. The maxima occur at the positions of the spin orbit resonances. Qualitatively similar curves are obtained at other positions in the ring. This curve is almost identical to that obtained when all vertical bends and the FS's are switched off. Furthermore, for amplitudes where the linear approach of SLIM provides a valid parametrization, the results of SPRINT are qualitatively very similar to the results of SLIM, except that the SLIM results only show first order resonances owing to the linearization. The trained eye will detect a periodicity in the energy reflecting the approximate four fold symmetry of the ring. The number of resonance peaks would be smaller with exact four fold symmetry. It is clear from this figure that even in a perfectly aligned ring, acceptable polarization could be obtained only over a very restricted part of the energy range even if a completely polarized beam were delivered at high energy. The broken curve shows the average angular deviation of \vec{n} from its average for particles distributed uniformly around the 3 sigma vertical and 1 sigma horizontal phase space ellipses.

Figure 9.4. The placement of four flattener snakes to make the straight sections in the North and the South transparent to spins on the closed orbit and the placement of a longitudinal and three radial Siberian Snakes in HERA.

9.4.2 HERA with Siberian Snakes

Siberian Snakes are not only essential for suppressing depolarization during acceleration but also help at fixed beam energy. In particular they are essential for suppressing spin flip effects due to resonance crossing as the energies of individual particles execute (slow) synchrotron oscillations [7]. Note that we ignored synchrotron motion in the last subsection precisely because synchrotron motion in the absence of the snakes can destroy the polarization. Snakes also stabilize the spin motion due to betatron oscillation since the orbital tunes can be chosen so as not to coincide with the fixed real spin tune generated by properly chosen snake layouts. Figure 9.5 shows the average angular deviation of \vec{n} for the FS layout described above and for the same orbit amplitudes as in figure 9.3 but with a snake layout suggested by V. Anferov [15], and previously studied in a slightly modified form for a flat ring in [7] (figure 51a). As shown in figure 9.4, there are snakes, with radial axes, near the vertical bends in the North and South, a snake with a radial axis near the midpoint of the West region, and a snake with a longitudinal axis near the midpoint of the East interaction region. The real spin tune is 1/2 independently of the energy and \vec{n}_0 is again vertical in the arcs and at the interaction points. No spin rotators have been included. The solid curve is for particles distributed uniformly around the 1 sigma vertical and 1 sigma horizontal phase space ellipses. Now we see that the dependence of the opening angle on energy is much smoother with a maximum in this energy range of about 0.72 radians and a minimum of about 0.3 radians. Even here, acceptable polarization could be obtained only over a restricted part of the energy range. The broken curve is for particles distributed uniformly around the 3 sigma vertical and 1 sigma horizontal phase space ellipses.

Figure 9.5 shows that installation of snakes is in itself not sufficient to ensure that an ac-

Figure 9.5. The average opening angle of the equilibrium spin distribution for energies between 814 and 822 GeV after the installation of the Siberian Snakes shown in figure 9.4. The two curves refer to particles with one sigma in the horizontal direction and one or three sigma in the vertical direction respectively.

ceptable polarization is attainable. As a next step we therefore used the following automatic filtering method aimed at inspecting all possible combinations of four Siberian Snakes and eliminating choices which do not satisfy certain criteria. The procedure works as follows:

- 1. Find all snake combinations for the ring which was flattened by FS's which lead to a spin tune of $\nu = 1/2$.
- 2. Compute the 1st order opening angle for the non-flat HERA proton ring and filter on small opening angles of the equilibrium spin distribution.
- 3. Compute the opening angle by 3rd and 5th order normal form theory for the snake combinations which are left after all these filters and filter on small opening angles if the normal form theory converges.
- 4. Compute the accurate equilibrium spin direction \vec{n} with stroboscopic averaging.

When we only use Siberian Snakes with vertical, radial or longitudinal axes, the best parallelism in a polarized beam in HERA is achieved by a longitudinal snake in the East and vertical snakes close to the three other interaction points. The polarization distribution over the one and three sigma vertical phase space ellipses with 1 sigma in the horizontal direction calculated using SPRINT is displayed in figure 9.6. Now the \vec{n} -axes are more tightly bundled and beam of higher polarization can be stored in HERA. We display results for this case since they are the best found so far, in spite of the fact that this arrangement will probably not be chosen in practice, since the average polarization in the arcs is not vertical. At first sight one might suspect that this case is effectively equivalent to that with a single longitudinal snake and that vertical snakes would therefore not improve the spin motion. However this suspicion is not supported by our calculations. Other choices of Siberian Snakes have been suggested,

Figure 9.6. The average opening angle of the equilibrium spin distribution for energies between 814 and 822 GeV after the installation of the snake arrangement found by filtering. The two curves refer to particles with one sigma in the horizontal direction and one or three sigma in the vertical direction respectively.

for example a solution with 45° snakes in the North and South [17]. These suggestions exhibited an even more disadvantageous behavior for the equilibrium spin distribution.

Further optimization might improve the situation but there are several other effects which might have serious consequences for the storage of polarized protons.

9.5 Further investigations

Apart from the obvious need to find adequate and practical snake schemes, to decide the best way to realize the FS's and to design and position the spin rotators needed to provide various \vec{n}_0 directions for the experiments at the interaction points, the following topics must be addressed.

- 1. Understand the effects of misalignments. Find cures. (The most important additional limitation to the polarization is likely to be the spread in the \vec{n} -axes caused by misalignments.)
- 2. Include linear and nonlinear synchrotron oscillations.
- 3. Determine the maximum allowed emittances.
- 4. Study the efficacy of the chosen snake scheme for controlling the spin 'equilibrium' during the adiabatic acceleration.
- 5. Evaluate the advantages of increasing the symmetry of the ring and the optic.
- 6. Determine the influence of the beam-beam effect.
- 7. Understand the influence of noise in power supplies.

- 8. Calculate with optical nonlinearities and optical coupling.
- 9. Evaluate the effect of intra-beam scattering, if any.
- 10. Investigate the relevance and feasibility of spin matching [14] and in particular the 'strong spin matching' proposed by K. Steffen [16].

References

- [1] D. P. Barber, K. Heinemann, G. H. Hoffstätter, and M. Vogt. Limits to the equilibrium proton spin polarization at high energy in HERA. DESY Report in preparation.
- [2] D. P. Barber. Prospects for polarized protons at HERA, In *International School of Nucleon Structure*, 1st Course: The spin structure of the nucleon, Erice, Sicily, August 1995. To be published by World Scientific Publishing Co. Ltd.
- [3] D. P. Barber. Possibilities for polarized protons at HERA. In *Prospects of spin physics at HERA*, DESY-Zeuthen, August 1995. DESY Report 95-200, November 1995.
- [4] G. H. Hoffstätter. Polarized protons in HERA. In *Proceedings of the DESY Accelerator Group Seminar*, St.Englmar, January 1996. DESY Report 96-05, May 1996.
- [5] K. Heinemann and G. H. Hoffstätter. A tracking algorithm for the stable spin polarization field in storage rings using stroboscopic averaging. DESY Report 96-078, May 1996. Accepted for publication in Physical Review E.
- [6] D. P. Barber, K. Heinemann, G. H. Hoffstätter, and M. Vogt. The phase space dependent spin polarization direction in the HERA proton ring at high energy. In The Proceedings of the 1996 European Particle Accelerator Conference, Sitges, Spain, May 1996.
- [7] V. Balandin, N. Golubeva, and D. P. Barber. Studies of the behaviour of proton spin motion in HERA-p at high energies. DESY Report M-96-04, February 1996.
- [8] L. Thomas. The kinematics of an electron with an axis. Philosophical Magazine, 3, 1 (1927).
- [9] V. Bargmann, L. Michel, and V. L. Telegdi. Precession of the polarization of particles moving in a homogeneous electromagnetic field. *Phys. Rev. Lett.*, 2, 435 (1959).
- [10] K. Heinemann. Thesis in preparation.
- [11] Ya. S. Derbenev and A. M. Kondratenko. Diffusion of particle spins in storage rings. Sov. Phys. JETP, 35, 230 (1972).
- [12] A.W. Chao. Evaluation of radiative spin polarization in an electron storage ring. *Nuclear Instruments and Methods*, **180**, 29 (1981).
- [13] D.P. Barber, K. Heinemann, and G. Ripken. A canonical 8-dimensional formalism for classical spin-orbit motion in storage rings. II Normal forms and the n-axis. Zeitschrift für Physik, C64, 143 (1994).
- [14] D.P. Barber, et al. A solenoid spin rotator for large electron storage rings. Particle Accelerators, 17, 243 (1985).
- [15] V. Anferov. Private communication. See also the Chapter 10.
- [16] K. Steffen. Strong spin matching with and without snakes: a scheme for preserving polarization in large ring accelerators. *Particle Accelerators*, **24**, 45 (1988).
- [17] E. Courant. Private communication.

10 HERA polarized beam hardware (820 GeV/c)

10.1 Flattening snakes

The lattice of the 820 GeV/c HERA proton ring has approximate four-fold symmetry and four straight sections as shown in Fig. 10.1. It seems natural to incorporate four Siberian snakes in the HERA ring according to the existing symmetry [1].

However, as shown in a DESY report [2], the vertical bends near the North and South experimental areas certainly make HERA into a non-flat ring and interfere with any standard snake configurations suitable for a flat ring. Therefore, we suggest installing four additional snakes [3] with radial axes in the North and South straight sections as shown in Fig. 10.1. These snakes, specially placed as shown later in Fig. 10.4, would compensate the vertical bends' effect on the spin and make these interaction regions spin transparent. To emphasize their purpose, we call these snakes "flattening snakes". Note that one could also cancel the effect of the vertical bends by putting a single longitudinal snake near the center of the straight section with vertical bends. However, this could be done only in the East straight section since the North and South straight sections are filled with collider detector hardware. Note that, if it were not possible to put a longitudinal snake near the East experimental area, two more flattening snakes could be installed in the East straight section or one could remove its vertical bends.

Figure 10.1. The layout of the hardware for the HERA polarized beam.

10.2 Depolarizing resonances in HERA

The maximum strength of the spin depolarizing resonances usually determines how many snakes are needed in an accelerator. Accelerating polarized protons to 820 GeV/c in HERA would require at least four full Siberian snakes. Four cold snakes could easily be located near each of the four long straight sections as shown in Fig. 10.1. In a ring with N_s snakes, the maximum strength of the tolerable intrinsic and imperfection depolarizing resonances ε_{max} is given by [4]

$$\varepsilon_{max} < N_s/5. \tag{10.1}$$

Thus, for four snakes, the HERA depolarizing resonance strengths should not exceed 0.8.

We estimated the strengths of the depolarizing resonances for a flat HERA using the program DEPOL [5]. Assuming the existing 25π mm-mrad polarized beam emittance, the calculated strengths of the intrinsic depolarizing resonances in HERA are plotted against γ in Fig. 10.2. The maximum strength is about 1.6, which is above the upper limit for the four snakes. The strengths of the imperfection resonance in HERA were calculated assuming the existing rms orbit error of 2 mm; these strengths are plotted in Fig. 10.3. Their maximum strength is about 3.6, which is above the upper limit for spin stability. Therefore, four snakes may not be adequate for maintaining the beam polarization in HERA. The DESY Polarization team suggested many ways to further study this difficulty which they first discovered using their very detailed spin tracking and stroboscopic averaging program SPRINT.

It now appears that the four normal Siberian snakes suggested for HERA are considerably less effective than the 6 snakes suggested earlier for the Tevatron; the benefit of an odd number of snake pairs was previously used in design studies [6, 1] (26 snakes at SSC and 6 snakes at the Tevatron) but perhaps not fully understood. Thus, with the existing 25π mm-mrad emittance and 2 mm rms orbit errors, it might be necessary to install 6 Siberian snakes in HERA to overcome the rather strong depolarizing resonances. Installing 6 snakes in HERA would probably require replacing some existing HERA dipoles with shorter higher fields dipoles to make appropriate spaces for the 2 extra Siberian snakes.

One should also consider various correction techniques to reduce the rms orbit error to perhaps 0.2 mm and the emittance to perhaps 5π mm-mrad. Simple scaling laws suggest that these corrections would allow the acceleration of polarized protons at HERA to 820 GeV; the ε_{int}^{max} would be reduced by about $\sqrt{5}$ to about 0.71 while the ε_{imp}^{max} would be reduced by about 10 to 0.36. For these values of $\varepsilon_{imp}^{max} = 0.36$ and $\varepsilon_{int}^{max} = 0.71$, the spin tracking programs may find spin stability at 820 GeV since the snakes would then dominate the spin motion according to Eq. (10.1). However, in the time frame of this Report, there is inadequate time to run these programs or to develop detailed techniques for reducing the rms orbit error or the emittance.

It was suggested during the study that, because of HERA's slow acceleration rate, the non-linear resonances, sometimes called snake resonances, may be much more significant at HERA than at the Tevatron. These resonances cannot be overcome by Siberian snakes; indeed, in some sense, they are caused by the snakes. Some special corrections may be needed for these snake resonances as discussed in Section 9. While the theory of these snake resonances, used in the tracking calculations of Section 9, appears reasonable, it has not yet been experimentally verified. There are only some results from a July 1996 experiment at IUCF, which are not yet fully analyzed.



Thus, the differences between the calculations of the several different groups of theoretical accelerator physicists appear to be most interesting and important, but not yet settled. Resolving these differences will require some additional time, some careful thought, and possibly some experimental data. One might try to determine experimentally if the overall effect of a snake resonance does or does not depend upon the acceleration rate.

10.3 Snake positions in HERA

Despite these possibly serious problems, we will describe a four Siberian snake configuration to possibly control the spin motion in an effectively flat ring. This could provide a preliminary estimate of the hardware costs in case some inexpensive solution is found to make the spin tune equal to 1/2 with 4 snakes and to provide stability against the higher order spin depolarizing resonances often called snake resonances. These snake resonances occur when an integer multiple of the vertical betatron tune is equal to a half integer. Several Siberian snake configurations could be considered including:

- Longitudinal snake at 0° and three radial snakes at 86.5°, at 180° and at 273.5°.
- Longitudinal snakes at 0° and 180° and two 45° snakes at 86.5° and at 273.5°.

In addition to these four normal Siberian snakes and the four flattening snakes discussed in Section 10.1, we also suggest installing four spin rotators in HERA, one on each side of H1 and ZEUS. This would allow the polarization direction to be changed at H1 and ZEUS while keeping the polarization vertical in the rest of the ring. The general layout of the Siberian snakes, flattening snakes, and spin rotators in HERA is shown in Fig. 10.1 along with one symbolic beam polarimeter. Fig. 10.4 shows the details of all four long HERA straight sections with the snakes and rotators installed in some existing free spaces of adequate length.

Figure 10.4. HERA straight sections with snakes and spin rotators.

Figure 10.4. (continued) HERA straight sections with snakes and spin rotators.

10.4 Snake designs

The snakes and spin rotators in HERA should be superconducting and would each require about 5 m of free space. Some possible designs of the normal Siberian snakes, the flattening snakes and the spin rotators are shown in Figs. 10.5, 10.6 and 10.7, respectively. Note that the Siberian snake design shown in Fig. 10.5 has a 45° spin rotation axis; its axis could be shifted to -45° by simply reversing the currents. Similar designs could be produced for snakes with 0° and 90° rotation axes; however, we could not design them in the time frame of this Report.

Figure 10.5. Possible design of a 45° normal Siberian snake for HERA.

Figure 10.6. Possible design of a flattening snake for HERA.

Figure 10.7. Possible design of a spin rotator for HERA.

10.5 Snake construction

In all three types of snakes (normal Siberian snakes, flattening snakes, and spin rotators), it might be wise to construct all the dipoles of identical laminations. This would simplify their design and fabrication and would also allow identical diameter cryostats. One candidate transverse design would be the HERA dipoles; another candidate would be the UNK-2 design. Using an existing transverse design would significantly reduce both the cost and time of the design and fabrication. We have assumed in our cost estimate that the dipoles would be built at DESY using the HERA dipole design; building the dipoles at IHEP-Protvino using the UNK-2 design might significantly reduce the cost.

We believe that operating either HERA-type or UNK-2-type superconducting dipoles at 5.5 T would be reasonable since all snakes would operate dc with no ramp to strain and heat the coils.

10.6 Cost Estimate

We estimate that the four normal Siberian snakes for HERA would cost about **DM 2.0 M**. The four flattening snakes would cost an additional **DM 2.0 M**; we estimate about **DM 1.5 M** for the four spin rotators around the collider detectors. We estimate the cost for power supplies to be **DM 0.7 M** and for cryogenic connections to be **DM 0.8 M**. The construction time for the snakes and spin rotators could be between 1.5 and 2 years.

References

- [1] SPIN Collaboration, "Acceleration of polarized protons to 120 GeV and 1 TeV at Fermilab", University of Michigan Report UM-HE 95-09, (1995).
- [2] D.P. Barber, "Prospects for polarized protons at HERA", International School of Nucleon Structure, Erice, Sicily, August 1995; D.P. Barber, "Possibilities for polarized protons at HERA", in Prospects of spin physics at HERA, DESY-Zeuten, August 1995, DESY Report 95-200; G. Hoffstätter, "Polarized protons in HERA", in Proc. of the DESY Accelerator Group Seminar, DESY Report 96-05, May 1996; V. Balandin, N. Golubeva and D.P. Barber, "Studies of the behaviour of proton spin motion in HERA-p at high energies", DESY Report M-96-04, May 1996.
- [3] J. Buon, "Spin-transparent vertical beam kicker", in Proc. of the Workshop on Polarized Beams at SSC, Ann Arbor 1985, AIP Conf. Proc. 145, 170 (1986).
- [4] S.Y. Lee and E.D. Courant, Phys. Rev. **D41**, 292 (1990).
- [5] E.D. Courant and R.D. Ruth, The acceleration of polarized protons in circular accelerators, BNL Report BNL-51270, (1980).
- [6] SPIN Collaboration, "SSC EOI-001", SSC Letter of Intent, 28 November 1990.

11 Transfer lines

There is a transfer line between each successive pair of accelerators at DESY. Transfer lines consist of three main elements: drift spaces, quadrupole magnets, and dipole magnets. Drift spaces and quadrupoles would have no effect on the polarization of a properly centered beam; however, the dipoles would cause the protons' spin to precess, which could change the beam polarization direction. The transfer lines cause no depolarization directly. However, a polarization loss would occur if the line's injected polarization were not aligned with the ring's stable spin direction; only the component of the injected polarization along the ring's stable spin direction would be preserved. A spin rotator should be inserted into each transfer line to correct the polarization alignment.

11.1 50 MeV line from the LINAC to DESY III

The polarization emerging from the LINAC should be vertical. If there were no partial Siberian snake in DESY III, then its stable spin direction would also be vertical. There are non-horizontal bends in the transfer line which move the proton beam from the LINAC level to the DESY III level. However, these bends would only slightly tilt the polarization; over 99% of the LINAC polarization would remain after injection into DESY III. Then no changes would be required in this line.

If there were a 5% partial Siberian snake in DESY III, then there would be a 10° tilt to the stable spin direction at injection; however, over 98% of the initial polarization would still remain without a spin rotator in the line. However, the necessary space exists for a 0.01 T·m solenoid, as shown in Fig. 11.1. It would probably be wise to install this small spin rotator for safety, especially since it would cost less than **DM 50k**.

Figure 11.1. 50 MeV transfer line from LINAC to DESY III.

11.2 7.5 GeV/c Line from DESY III to PETRA

The 7.5 GeV/c transfer line would begin with vertically polarized protons extracted from DESY III. The most likely option for PETRA would have two Siberian snakes on at injection. This would give a vertical stable spin direction in PETRA at injection. Then the transfer line would require no spin rotator, because the only vertical bends in the transfer line are opposite and have no horizontal bends between them, as shown in Fig. 11.2.

Figure 11.2. 7.5 GeV/c transfer line from DESY III to PETRA (vertical scale expanded).

11.3 40 GeV/c line from PETRA to HERA

Both PETRA Siberian snakes would probably be on during extraction; therefore, the 40 GeV/c line would begin with vertically polarized protons extracted from PETRA. HERA would have four normal Siberian snakes on at injection; therefore, it would need vertically polarized injected protons to match its vertical stable spin direction. However, there are many non-horizontal bending magnets in the 40 GeV/c line that would rotate the spin away from the vertical; the transfer line spin direction at the HERA injection point would have components:

$$\hat{v} = 0.807 \quad \hat{r} = 0.324 \quad \hat{l} = -0.494 \ . \tag{11.1}$$

Thus, with no rotator, only 80% of the polarization emerging from PETRA would be transmitted to HERA. To obtain the maximum polarization in HERA, a spin rotator would be needed in this 40 GeV/c line. There are several positions where a spin rotator could be fit into this line. Three options are shown in Fig. 11.3; for each option a spin rotation of 38.6° would be required. The length of each straight section and its required spin rotation axis components are shown in Table 11.1.

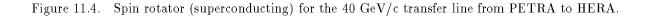
Figure 11.3. 40 GeV/c transfer line from PETRA to HERA (vertical scale expanded).

Table 11.1. Required spin rotation axis direction in the 40 GeV/c transfer line.

Position	Space available	\hat{v}	\hat{r}	î
1	9.1 m	-0.039	-0.892	-0.454
2	7.9 m	-0.466	0.118	0.877
3	$23.0 \mathrm{m}$	-0.469	-0.644	0.604

11.4 Spin rotator construction

The 40 GeV/c spin rotator could be built of superconducting dipoles with the same aperture as the superconducting HERA snakes and rotators. A possible design is shown in Fig. 11.4. This superconducting rotator would require either a helium transfer line from the main HERA helium line or a helium storage dewar which could be filled perhaps once a week. Alternately one could use a warm rotator with a larger but similar design; this would need no helium but would consume much more power. The choice should be based on minimizing the total cost of construction plus operation for perhaps 5 years.



11.5 Cost estimate

We estimate that the warm solenoid spin rotator in the 50 MeV line would cost **DM 50 k**. The cold spin rotator in the 40 GeV/c line would cost about **DM 450 k**, including power supplies and cryogenic connections.

12 Polarimeters

Any spin experiment must have an accurate measurement of the beam and target polarization. Polarimeters are also necessary for monitoring the polarized beam acceleration and optimizing the output polarization. Both absolute and fast relative polarimeters could be used in a polarized beam acceleration project. The main problem is to find a reaction with a large cross-section, whose analyzing power is large and either measured or calculable. Moreover a polarimeter should be simple and reliable and should allow a fast polarization measurement without degrading the polarized beam.

The low energy polarimeters discussed in the following section are fairly simple and work rather well. These polarimeters would include a 20 keV source polarimeter, a 50 MeV Linac polarimeter and a $7.5~{\rm GeV/c~DESY~III}$ polarimeter.

For high energy protons, an ideal polarimeter does not yet exist. One proposed polarimeter uses proton-proton elastic scattering at very small t, where the Coulomb and hadronic amplitudes interfere. Both this Coulomb-Nuclear Interference (CNI) polarimeter and a Primakoff polarimeter have already been used in Fermilab experiments [1, 2]; a CNI polarimeter may provide an absolute calibration.

One could also use an inclusive pion production polarimeter at high energies and an AGS-type relative polarimeter. Moreover, the 820 GeV *p-p* elastic experiment described in Section 3, could certainly give an absolute calibration of the beam polarization as was done at the ZGS and then the AGS.

12.1 Source Lyman- α polarimeter

The source "Lyman- α " polarimeter is based on the asymmetry in the hyperfine level populations of metastable H(2S) atoms [3]. The beam leaving the ionizer of the polarized H⁻ ion source contains a small fraction of protons; during polarization measurements, they could be used to create metastable hydrogen atoms by charge exchange with Na vapor. A "spin filter", consisting of a 580 G longitudinal field and a 15 V cm⁻¹ transverse electric field, then quenches the atoms in the two lower energy (spin-down) metastable hyperfine states by mixing with the ground state. The polarization is then measured by detecting the Lyman- α 122 nm light emitted by the surviving spin-up metastable atoms in a relatively strong electric field. Very high count rates of about 10^6 to 10^7 s⁻¹ per microampere of polarized proton current would permit rapid measurement of the polarization.

The absolute accuracy of a Lyman- α polarimeter is not high, due to its systematic errors. However, it would allow fast measuring and tuning of the source polarization with high relative precision. The estimated **DM 50** k cost of a Lyman- α polarimeter is included in the source budget.

12.2 50 MeV LINAC polarimeter

The 50 MeV polarimeter proposed here would be similar to the ZGS LINAC polarimeter [5]. If the LINAC is upgraded to 160 MeV, then the polarimeter could be more similar to the AGS LINAC polarimeter which operated at 200 MeV [4]. Either polarimeter would quickly give a precise absolute measurement of the beam polarization before injection into DESY III. The 50 MeV polarimeter would detect 50 MeV protons, which were elastically scattered from a carbon target at a 55° laboratory angle. At this scattering angle, the analyzing power is about 85% and the cross section is 10 mb/sr [6]. The polarimeter would consist of two left-right symmetric 3-counter scintillator telescopes looking at a thin carbon target. All but elastic events would be ranged out prior to the last scintillator. The first two counters would be 3 mm thick scintillators giving a total energy loss of about 20 MeV. An energy absorber composed of 5 mm polyethylene sheets would be installed after the second counter. The elastic protons would leave the absorber with a kinetic energy of about 13 MeV and, after a 35 cm flight path, would be stopped in a third counter. A combination of detected pulse height and time of flight would cleanly separate the elastic events from the background. The measured left-right count asymmetry A_m would give the beam polarization P_B using $P_B = A_m/A_N$ where A_N is the analysing power. A few percent measurement would take about a minute.

The cost estimate for the 50 MeV polarimeter's detectors, electronics and vacuum hardware is **DM 200 k**.

12.3 Inclusive pion polarimeter

We have also considered pion production as a possible reaction to measure the high energy proton beam polarization. Measurements at 11.75 GeV/c [11] and at 200 GeV [2] found a large analyzing power A_N for inclusive pion production in p-p collisions at large x and P_{\perp} above 0.7 GeV/c. An inclusive polarimeter is also being considered for RHIC [12]. Fig. 12.1 shows the measured [2] analyzing power at 200 GeV/c plotted against the Feynman variable x_F , which is the ratio of the pion's cm longitudinal momentum to the maximum cm longitudinal momentum. For P_{\perp} above 0.7 GeV/c, the asymmetries increase from 0% at $x_F = 0.3$ to 28% at $x_F = 0.7$; furthermore, A_N appears to be independent of the polarized beam momentum. Moreover, the ZGS data [11], which were taken with both liquid hydrogen and deuterium targets, show no dependence on target nuclei.

Figure 12.1 Proton-proton inclusive analyzing power at 200 GeV plotted against x_F for charged pion production with transverse momenta below and above 0.7 GeV/c [2].

At HERA or PETRA, one could measure the left-right asymmetry in inclusive negative particle production; this is certainly dominated by π^- production so that particle identification is essentially unnecessary. Therefore, the apparatus could be rather simple and could consist of a carbon fiber target, one or two dipole magnets and four small scintillation counters. The figure of merit for the polarimeter is proportional to the event rate and the analyzing power squared; the maximum value occurs near $x_F = 0.6$, where $A_N = 0.21$. The spectrometer's angle and momentum would then depend on the beam energy. For HERA's 820 GeV/c momentum, the outgoing pion's momenta at $P_{\perp} = 0.8$ GeV/c would be 492 GeV/c and its angle would be 1.63 mrad; at 40 GeV/c, they would be 24 GeV/c and 33 mrad, respectively.

Such a polarimeter could be placed near the HERA East Hall or in the West straight section in PETRA. Clearly much more detailed design work is required on this inclusive polarimeter, which is shown in Fig. 12.2, but it probably would work well at both 40 GeV/c and 820 GeV/c.

Using a 1 μ m thick carbon band target, the luminosity would be $\mathcal{L}=1.2\cdot 10^{34}~\rm cm^{-2}\,s^{-1}$ for a 4.4 \cdot 10¹⁷ s⁻¹ polarized beam current in HERA. The invariant cross section at $P_{\perp}=0.8~\rm GeV/c$ is about 41.6 μ b GeV⁻² at 820 GeV/c. Then the counting rate per second would be

$$R = \mathcal{L} \cdot E \frac{d^3 \sigma}{dP^3} \left[\frac{\mu b}{GeV^2} \right] \cdot \Delta \Omega \cdot P_{lab} \cdot \Delta P_{lab}. \tag{12.1}$$

For a typical $\Delta\Omega = 10^{-6}$ sr and $\Delta P_{lab}/P_{lab} = 5\%$, we obtain $R = 6.2 \cdot 10^3$ events s⁻¹. The number of events N needed for a $\pm 5\%$ beam polarization measurement, with an 80% beam polarization, and $A_N = 0.21$, is given by

$$N = (0.8 \cdot 0.21 \cdot 0.05)^{-2} = 1.4 \cdot 10^4 \text{ events.}$$
 (12.2)

The time required for this 5% measurement would be about 2.3 seconds. This polarimeter would certainly destroy the beam and could not be used during normal HERA operation.

To decrease the beam losses in HERA, one might use an unpolarized gas jet target with a luminosity of 10^{31} cm⁻² s⁻¹. One would then get 5 events s⁻¹; the measuring time for a $\pm 5\%$ measurement would then be about 50 min, which is reasonable for a data run.

The estimated cost of each inclusive polarimeter for PETRA and HERA is **DM 600 k**.

Figure 12.2. Possible inclusive polarimeter.

12.4 CNI polarimeter

Because of the weak energy dependence of the analyzing power A_N for p-p elastic scattering in the Coulomb Nuclear Interference region [8, 9], measuring the p-p elastic scattering asymmetry seems a good way to obtain the proton beam polarization near 40 GeV/c and 820 GeV/c. Despite the small CNI analyzing power of about 4%, the proton-proton elastic scattering cross-section is large near |t| = 0.003 (GeV/c)². Moreover, p-p elastic scattering at small t can be detected with a simple apparatus with no magnets for momentum analysis; in addition, the CNI analyzing power can be calculated theoretically with some reliability [8, 10]. Experimental measurements of the CNI analyzing power were made by E-704 using a 200 GeV hyperon-decay polarized proton beam at Fermilab [1]; the data are shown in Fig. 12.3. The statistical precision was limited by the low beam intensity; however, the measured A_N is consistent with the prediction.

Since identification of elastic *pp* events is fairly simple, the polarimeter apparatus would include a hydrogen gas jet target and two detector arms, each consisting of a commercially available silicon strip detector and two scintillation counters.

The |t| range for the CNI polarimeter could be obtained by requiring the CNI analyzing power to be more than 1% and then optimizing the background conditions. This suggests a |t| range from 0.002 to 0.011 (GeV/c)²; in this range the mean A_N value is about 3.9% and the cross section is about 0.83 mb. By using a dense unpolarized jet target with thickness $7 \cdot 10^{14}$ cm⁻² one could obtain a rather high luminosity of $\mathcal{L} = 3 \cdot 10^{32}$ cm⁻²s⁻¹ in the 820 GeV/c HERA whose polarized beam circulating current would be about $4.4 \cdot 10^{17}$ s⁻¹.

Figure 12.3. Analyzing power in pp-elastic scattering at $E_{lab} = 200 \text{ GeV} [1]$

To make a $\Delta P/P = \pm 5\%$ polarization measurement with the CNI polarimeter one must collect about $8 \cdot 10^5$ events. For a vertical acceptance of $\Delta \phi \simeq 2.3^{\circ}$ the expected event rate would be $1.7 \cdot 10^3 \ s^{-1}$, which would allow a 5% measurement in about 10 minutes.

The estimated cost of each CNI polarimeter for PETRA and HERA is about **DM 300** k.

12.5 Relative AGS-type polarimeter

Internal polarimeters for DESY III and possibly PETRA and HERA could be similar to the AGS internal polarimeter [4], which is shown in Fig. 12.4; its target was a nylon fishline, typically 0.1 mm in diameter. On each side of the beam, at 77°, was a telescope consisting of 3 scintillator detectors. Wedge-shaped aluminum absorbers were installed to allow the final thickest detector to stop the relatively slow (200 MeV) elastic protons. The resulting large signal and proper timing in the coincidence helped to pick out the elastic protons. The effective analyzing power was about 2.3% at 13 GeV/c, which is about half of the value for pure elastic p-p scattering. Note that this device is not an absolute polarimeter. The final, defining detector in each arm was 5 cm \times 7.5 cm (h \times v) and was located 114 cm from the target. The AGS circulating polarized beam current was typically 1 mA, and the duty cycle was typically 100 ms each 2 s; measurements with errors of a few percent took about 10 minutes.

 ${\bf Figure~12.4.~Relative~polarimeter~at~AGS}.$

If 1% of the DESY III circulating beam of about 10^{12} passed through a 0.1 mm thick CH₂ target, and the defining detectors were 1 cm \times 4 cm (h \times v) at 1 m from the target and at 77° from the beam direction, then the p-p elastic event rate would be about 10 MHz. Including a duty factor of 20% and an effective analyzing power A_N of 6% (half of the elastic p-p power), a 1% measurement of beam polarization would take less than a minute. Another possible scattering mechanism is quasi-elastic scattering from the nucleons in carbon; the measured [7] quasi-elastic A_N may be as high as 40% of the elastic A_N . At PETRA and HERA, A_N would be smaller except in the CNI region, but this Relative polarimeter may still be quite useful.

The cost of each Relative AGS-type polarimeter is estimated to be **DM 200 k** and the production time is estimated to be 12 months.

12.6 p-p elastic polarimeter

One could use the proposed East Hall elastic scattering experiment to calibrate itself and the other HERA polarimeters; this "self calibration" technique was used at the ZGS [5] and then at the AGS [4]. One would simultaneously measure the "left-right asymmetry" (A_N) in 820 GeV/c p-p elastic scattering in both the beam "direction" and the target "direction". Assuming rotational invariance of space, one could then calibrate the beam polarization against the polarization of the Michigan Jet target which would itself be calibrated using its maser polarimeter, as described in Section 3. The cost of this experiment was estimated at about **DM 2.5 M**; using it as a polarimeter would not increase its cost.

12.7 Cost estimate summary

The polarimeters which might be used in each accelerator and their estimated costs are summarized in Table 12.1.

Accelerator	Energy	Polarimeter	Cost	Comment
Source	$20 \mathrm{keV}$	Lyman- α	DM 50 k	charged to source
RFQ	$750~\mathrm{keV}$	_		
LINAC	$50~\mathrm{MeV}$	p-Carbon	DM 200 k	
DESY III	$7.5~\mathrm{GeV/c}$	Relative AGS-type	DM 200 k	
PETRA	$40~{ m GeV/c}$	Relative AGS-type	DM 200 k	
		CNI	$\mathrm{DM}\ 300\ \mathrm{k}$	
		Inclusive??	$\mathrm{DM}\ 600\ \mathrm{k}$	use 50% of cost
		Total	DM 800 k	
HERA	$820~{ m GeV/c}$	Relative AGS-type	DM 200 k	
		CNI	$\mathrm{DM}\ 300\ \mathrm{k}$	
		Inclusive	$\mathrm{DM}\ 600\ \mathrm{k}$	
		p- p elastic	DM 2.5 M	charged to experiment
		Total	DM 1.1 M	

Table 12.1. An Estimate of the costs for the polarimeters.

References

- [1] N.Akchurin et al., Phys. Rev. **D48**, 3026 (1993).
- [2] D.L. Adams et al., Phys. Lett. **B264**, 14 (1991).
- [3] A.N. Zelenskii et al., Nucl. Instr. and Meth. **A245**, 223 (1986).
- [4] F.Z. Khiari et al., Phys. Rev. **D39**, 45 (1989).
- [5] T. Khoe et al., Part. Accel. 6, 213 (1975).
- [6] L.N. Blumberg et al., Phys. Rev. 147, 812 (1966);
 M.P. Fricke et al., Phys. Rev. 156, 1207 (1967).
- [7] J. Bystricky et al., Journale de Physique, Colloque C2, supplement au n02, Tome 46, C2-483 (1985).
- [8] B.Z. Kopeliovich and L.I. Lapidus, Sov. J. Nucl. Phys. 19, 114 (1974).
- [9] SPIN Collaboration, Acceleration of Polarized Protons to 120 GeV and 1 TeV at Fermilab, University of Michigan Report UM HE 95-09 (1995).
- [10] A.D. Krisch and S.M. Troshin, Estimate of elastic proton-proton polarization at small P_{\perp}^2 near 1 TeV, UM HE 95-20.
- [11] W.H. Dragoset et al., Phys. Rev. **D18**, 3939 (1978).
- [12] T. Roser, private communication.

13 Polarized proton beam accumulation

If a DESY polarized H⁻ source (either an OPPIS or ABS) were assumed to have only the existing maximum polarized current of 1.6 mA, compared to the present 60 mA unpolarized source current, then the normal DESY injection and acceleration scheme would yield a correspondingly lower HERA intensity. This section will first briefly describe the present beam accumulation and acceleration method used in the LINAC, DESY III, PETRA, and HERA complex. It will then discuss some ideas for increasing the final HERA polarized proton current, the expected problems with each idea, and the additional hardware needed.

13.1 Present scheme for beam accumulation and acceleration

The DESY unpolarized source provides about 60 mA of H⁻, which is accelerated to 50 MeV by the LINAC. Because of losses in the LEBT, RFQ, and LINAC, only about 10 mA is actually injected into DESY III using 10-turn H⁻ strip injection, which lasts about 33 μ sec. The cycle time for DESY III is about 4 sec; hence the LINAC must pulse at 0.25 Hz. This beam in DESY III is captured into 11 bunches and then accelerated to about 7.5 GeV/c. A bunch separation of 28.8 m is established in DESY III and is maintained up to 820 GeV/c. DESY III's beam current is about 180 mA (1.2 10^{12} protons) at 7.5 GeV/c. In DESY III, the longitudinal emittance of the beam only fills about 1/10 of the available bucket space.

This 7.5 GeV/c beam is then transferred to PETRA by a "bunch to bucket" transfer using single turn extraction/injection. Since PETRA is just above transition energy at injection, dispersion is introduced to produce a stable beam; this makes the buckets in PETRA much smaller than in DESY III, but just large enough to accommodate the longitudinal emittance of the DESY III bunches.

Six cycles of 10 bunches from DESY III get transferred to 60 bunches in PETRA. Then PETRA accelerates to 40 GeV/c in about 2.4 min, with about 100 mA (4.8 10¹² protons) at the top of the ramp. Three PETRA cycles of 60 bunches then fill 180 buckets (out of 210) in HERA. The extra buckets are left empty so that the injection kickers have time to turn off after the single turn injection. There is also a longitudinal phase rotation in PETRA so that the bunches which are long in time and short in momentum spread are turned into bunches which are short in time and large in momentum spread to fit into the very short time buckets in HERA. The HERA bunches must be short to maximize luminosity, since the HERA positron bunches are short. This HERA beam is then accelerated to 820 GeV/c in about 15 min for a final current of about 70 mA (9.2 10¹² protons). It is believed that the available transverse phase space in HERA is full. The evidence for this is:

- The transverse 2σ emittance can vary between $20-25\pi$ mm-mrad,
- the beam lifetime at injection is about 6 hrs at 20π mm-mrad, and drops to 2-3 hrs at 25π mm-mrad.
- at 70 GeV, where the emittance has been damped substantially, the beam lifetime is several hundred hours.

13.2 Increasing the polarized beam intensity

The possibilities for increasing the polarized beam intensity in HERA can be grouped into three general categories:

- Beam accumulation in DESY III: longer duration (i.e. more turns) H⁻ strip injection into DESY III, as well as possibly stacking several sets of strip injected beams.
- Beam stacking (longitudinally and/or transversely) in PETRA and/or HERA.
- An electron-cooled 50 MeV to 1 GeV accumulator ring for injection into DESY III.

13.2.1 Polarized beam accumulation in DESY III

Currently the LINAC supplies a 10 mA beam for 33 μ sec for 10 turn H⁻ injection into DESY III. To increase the number of injection turns one should take full advantage of the possible increase in phase space density for polarized beam. If the present injected beam losses, of about 70% in LEBT and about 10% in the RFQ, were current independent, then, with the present 1.6 mA OPPIS source, one could expect only 300 μ A of polarized beam injected into DESY III. Then injecting polarized beam for about 300 turns would yield the present circulating unpolarized beam in DESY III; however, this is probably not feasible for the following reasons:

- This would require the source, RFQ and LINAC to pulse for about 1 msec; the present LINAC can pulse for at most 100 μs at 3 Hz. Increasing the LINAC pulse duration would be difficult.
- Since the transverse emittance increases for each pass through the DESY III stripper foil, there is a point of diminishing returns for multiturn injection. This emittance increase per pass through the foil has not yet been measured well.
- The current DESY III injection kicker scheme, where injection occurs at the top of the injection kicker $\cos(\omega t)$ waveform, is already at its limit with 10 turn injection. This system would require an upgrade for injection of many more turns.

Therefore, totally compensating for the lower polarized source current by simply injecting into DESY III for many more turns may not be possible. However, one should certainly try to extend this injection time as much as possible.

Depending on the longitudinal and transverse emittances of the polarized injected beam, it may be possible to do some sort of multiturn H⁻ injection combined with stacking in one of the planes. This has the advantage that the previously injected beam, while circulating in DESY III, would be away from the foil when further injection occurs; also one could perhaps reduce the LINAC pulse duration, but perhaps increase its duty factor. One possibility is to continuously change the LINAC energy during injection, as well as the dipole fields in DESY III, so that the injected beam strikes the foil for a fixed (and preferable short) number of times before its orbit moves away from the foil. For this to work, the horizontal emittance should be much smaller than the acceptance of DESY III, so that there is room to stack, and also that the final DESY III stacked beam fits into the acceptance of PETRA. It would probably be straightforward to ramp the energy of the LINAC slightly during injection, and ramping the DESY III dipoles a small amount is easy. One thing to consider is the beam

lifetime at 50 MeV in DESY III, which is very short. It should be emphasized that there has been no calculations yet on this possibility. In order to answer questions about stacking in any of the rings, one first has to make an estimate of the properties (i.e. emittances) of the beam coming out of the LINAC.

Other stacking schemes may be possible. Note that for longitudinal stacking, the longitudinal emittance of the stacked DESY III beam must be small enough to fit into the much smaller longitudinal acceptance of PETRA.

It has been suggested that studies be done to learn more about beam accumulation possibilities in DESY III. These studies may be relatively easy to arrange, since during HERA running, DESY III is mostly idle. These studies could be valuable in answering questions about the source to DESY III system. One could simulate a polarized source either by collimating or by running one of the two existing unpolarized sources at a much lower current.

13.2.2 Stacking in PETRA and/or HERA

Estimating the beam stacking gains in either PETRA or HERA will require a good estimate of the properties of polarized beam coming out of the LINAC; this has not yet been made. In either ring, stacking will only be possible if the incoming beam emittance is much smaller than the ring's acceptance. The following points should be considered:

- Both the PETRA and HERA injection systems are designed for single turn injection. Multi-turn stacking injection would require an upgrade of the injection hardware.
- Any stacking scheme must consider injection errors. A large error in the beam placement at injection could quickly spread a small emittance beam over much of the available phase space, causing phase space dilution.
- Stacking will be limited by the beam lifetime at injection. The lifetime for 7.5 GeV/c protons in PETRA is about 20 min, while the lifetime for 40 GeV/c protons in HERA is at least 2-3 hrs. For polarized protons with a small emittance these lifetimes could increase substantially.

It may become necessary to extend the above mentioned DESY III beam studies to PETRA. However, since PETRA has other duties besides filling HERA, these studies would be more difficult to arrange.

13.2.3 Accumulator booster option

Two options are presently being considered for upgrading injection into DESY III:

- a 160 MeV upgrade of the LINAC by adding an additional tank; this would increase the number of DESY III turns during the 100 μ s LINAC pulse by the circulation time ratio of about 5:3.
- addition of a 50 MeV to 1 GeV/c booster synchrotron with multiturn H⁻ strip injection; this could increase the polarized beam intensity.

One might install an electron cooler in this new ring. Then beam could be accumulated for many turns since the emittance growth could be "shrunk back" with the cooling. One possible scheme would be to inject for as long as possible and then cool the beam; next one

would inject additional beam and repeat the process. Beam cooling at 50 MeV would take less than 1 second, which is about the same time as the present maximum LINAC rep rate of 1 Hz. One might then be able to put as much beam into this ring as DESY III currently gets at injection, or more, since longitudinal instabilities in DESY III caused by space charge effects would be substantially reduced if the injection momentum were 1 GeV/c. It may then be possible to have exactly the same polarized beam current in HERA as unpolarized beam current, with an increased overhead time for polarized beam accumulation. Another possible advantage to this scheme is that it may not require substantial (if any) upgrading of the present LINAC RF/cooling hardware.

This booster is in its very initial stage of design. There is presently no plan to install an electron cooler in this booster. It should be emphasized to the designers that electron cooling could solve many of the polarized beam luminosity problems for HERA; thus the electron cooling option should not be "designed out".

13.3 Conclusions

Polarized beam accumulation for HERA is clearly important. One should estimate the properties of the beam emerging from the DESY LINAC for a possible polarized proton source; this might indicate how much room exists in phase space for stacking. Beam accumulation in DESY III might be the easiest from a technical standpoint; thus, such DESY III studies, with a reduced intensity unpolarized source, seem valuable.